Environmental Science Nano

Accepted Manuscript

This is an *Accepted Manuscript*, which has been through the Royal Society of Chemistry peer review process and has been accepted for publication.

Accepted Manuscripts are published online shortly after acceptance, before technical editing, formatting and proof reading. Using this free service, authors can make their results available to the community, in citable form, before we publish the edited article. We will replace this *Accepted Manuscript* with the edited and formatted *Advance Article* as soon as it is available.

You can find more information about *Accepted Manuscripts* in the Information for Authors.

Please note that technical editing may introduce minor changes to the text and/or graphics, which may alter content. The journal's standard Terms & Conditions and the Ethical guidelines still apply. In no event shall the Royal Society of Chemistry be held responsible for any errors or omissions in this *Accepted Manuscript* or any consequences arising from the use of any information it contains.

ROYAL SOCIETY OF CHEMISTRY

rsc.li/es-nano

Nano impact

Halloysite nanotubes (HNTs) are one-dimensional nanomaterials with tubular structure and abundant deposit worldwide. In this article, recent progress in fabrication and applications of HNTs-based composites are briefly reviewed. This is the first review paper to discuss the special applications of the inexpensive nanomaterial to address the problems of wastewater treatment. Critical issues and future prospects with respect to the practical applications in various types of wastewater recycling or treatment will be presented. We believe, HNTs with highly unusual geometry and surface chemistry will be potentially and effectively employed in massive removal of contaminants from wastewater with various ways in industries.

Environmental Science: Nano Accepted Manuscript

Recent advance of halloysite nanotubes derived composites in water treatment

Liang Yu [a, c], Huixian Wang [b], Yatao Zhang [a]*, Bin Zhang [a], and Jindun Liu [a]

[a] *School of Chemical Engineering and Energy, Zhengzhou University, Zhengzhou 450001, China*

[b] *School of Civil Engineering and Communication, North China University of Water Resources and Electric Power, Zhengzhou 450045, China*

[c] *Department of Chemical Engineering, Hiroshima University, 1-4-1 Kagamiyama Higashihiroshima, 739-8527, Japan*

*Corresponding author:

Tel: +86-371-67781734; Fax: +86-371-67739348

E-mail: zhangyatao@zzu.edu.cn

Environmental Science: Nano Accepted Manuscript

Abstract

Halloysite nanotubes (HNTs) are natural occurring clay mineral with nanotubular structures and have found increasing potential applications in industrial fields. Here, after a brief introduction of the general structure, main properties and newly emerging applications of HNTs, particular attention is paid on HNTs-derived applications in water treatment. We mainly review the recent progress toward applications of HNTs-derived nanocomposites in heavy metal ions, dyes or organic pollutants removal from wastewater and HNTs-contained membranes for water filtration. The HNTs-derived composites exhibit superior properties for water treatment in various ways and are promising to be used in practical applications. Finally, we summarize the predominant mechanisms acted in the applications of water treatment and future prospects are discussed.

Environmental Science: Nano Accepted Manuscript

1. Introduction

Halloysite was first described in 1826 by Berthier as a dioctahedral 1:1 clay mineral of kaolin group and the extensive research began from 1940s.[1,2] Halloysite was widely found in both weathered rocks and soils worldwide. Countries like China, New Zealand, and Brazil deposit considerable amount of halloysite. The particles of halloysite adopt different morphologies including short tubular, spheroidal and platy shapes due to the variety of crystallization and geological occurrence. However, the predominant morphology of halloysite clay is elongated tubule, generally called halloysite nanotubes (HNTs). In this paper, "HNTs" is used hereafter for abbreviation to demonstrate the tubular halloysite clay, regardless of hydration and dehydration status, unless otherwise stated. Typically, the external diameter, lumen, and length of HNTs are 50-100 nm, 10-30 nm, and 100-2000 nm, respectively. This property enables potential applications as nanoscale support or functionalized nanomaterials and put HNTs back in the spotlight with the rapid development of nanoscience and nanotechnology in the past decade. Some other interesting characteristics of HNTs such as different internal and external surface chemistry, good biocompatibility and high mechanical strength will be discussed in detail in the following part. It is due to such a fact that HNTs have found increasing potential applications in increasing fields as reported in recent years. A survey of open publications in terms of "halloysite" to the past 10 years is presented in Fig. 1. These data, obtained based on a SciFinder Scholar search, obviously describe the increasing attention on halloysite, particularly in the past 4 years. Hence, an increasing number of publications are expected in the

Environmental Science: Nano Accepted Manuscript

upcoming years.

Some interesting applications of HNTs were mainly focused on controlled/sustained release of drugs or bioactive molecules,[3-10] cosmetics,[11] medical implants,[12,13] cancer cell isolation,[14,15] and tissue engineering scaffolds,[16-19] nanoreactors or nanotemplates[20-22] due to the cellular nontoxicity, environmental friendliness, biocompatibility properties and as well as the lumen space. Particularly, tremendous studies focused on HNTs/polymer composites as an inexpensive and low-tech alternative which provide exceptional mechanical, thermal and biological properties. Several researchers have reviewed the recent progress toward the development of HNTs/polymer nanocomposites with their particular interests. Du et al. (2010) [23] briefly reviewed newly emerging applications of HNTs, emphasizing the fabrication of HNTs/polymer nanocomposites with remarkable reinforcing effects, enhanced flame retardancy and reduced thermal expansion properties. Lvov and Abdullayev (2013) [24] presented recent studies on HNTs/polymer nanocomposites especially for the applications of controlled release. Liu and coworkers (2014) [2] introduced recent advance of HNTs/polymer nanocomposites from preparation, characterization to properties. In fact, besides the applications mentioned above, HNTs were always functionalized for other various important applications. Previously, we have explored diverse useful applications of functionalized HNTs, such as immobilization of enzyme or antibacterial agents, proton conduction, super-absorbent resin etc.[25-35]

With the rapid development of economy, the problem of pollution and shortage of water resource is becoming more serious, especially in developing countries. Among

Environmental Science: Nano Accepted Manuscript

all the causes of water pollution, heavy metal ions, dyes, pesticide and some other organic pollutants take up a great proportion. In this regard, it is of significance to study approaches or inexpensive materials for wastewater treatment. As reported in very recent years, HNTs or HNTs-based materials have also found many useful applications in treatment of drinking water or industrial waste water. In addition, so far, no review articles of HNTs-based materials have been published paying particular attention on the applications of water treatment. Therefore, a comprehensive and critical review on this topic is necessary to provide a better understanding for the HNTs-derived applications in water treatment. Accordingly, in this article, after briefly inducing the general structure and main properties of HNTs, we review the applications of HNTs derived nanocomposites in fields of water treatment, paying special attention to heavy metal or dyes removal from wastewater, membrane separation for water filtration.

2. General structure and main properties of halloysite nanotubes

HNTs, as rolled aluminosilicate sheets, have a similar theoretical formula to kaolinite expressed as $Al_2Si_2O_5(OH)_4 \cdot nH_2O$ where n equals 2 and 0 for hydrated and dehydrated HNTs, respectively. Generally, the presence, or history, of interlayer water in HNTs is one of most significant characteristics to distinguish HNTs from kaolinite.[37] The hydrated state (also called HNTs-10 Å) can transform into dehydrated state (HNTs-7 Å) irreversibly even under ambient conditions (of temperature and humidity) or by moderate heating. It is therefore difficult, if not impossible, to handle HNTs-10 Å without inducing alteration in its hydration status.[37] As the dominant

Environmental Science: Nano Accepted Manuscript

morphology of halloysite, HNTs present different appearances, long or short, thin or stubby, as shown in Fig. 2a. HNTs have layered, well crystallized structure consisting of aluminum oxide octahedrons in the inner layer and silicon dioxide tetrahedrons in the outer layer (Fig. 2b). Fig. 2c presents the typical XRD patterns of HNTs powders including HNTs-10 Å and HNTs-7 Å states. Broad peaks corresponding to 9.934 Å and 7.326 Å are respectively found in HNTs-10 Å and HNTs-7 Å assigned to the first order (001) basal reflections due to the less ordered multilayer structure. The high intensity and/or sharp peaks around 4.4 Å in either sample are indicative for halloysite, [24, 37] where just a quite weak and/or broad peak is observed for kaolinite sample.

HNTs show a moderate BET surface areas ranging from 22.1 to 81.6 m^2/g with a 10.7-39% lumen space and a relatively lower density of 2.14-2.59 g/cm^3. [38-40] The big lumen space provides advantages for the loading of active substances under vacuum by immersion in an appropriate solution. In addition, the lumen space is possibly to be enlarged by selective acid corrosion of aluminum oxide as described by Lvov (see Fig. 3). [41] The outer surface of HNTs shows different chemical and electrical properties with the inner surface because of the different crystal structures. The outer surface possesses a relatively lower hydroxyl group density (Si-OH) and negative charge, while the inner surface has abundant hydroxyl groups (Al-OH) and positive charge. In fact, the outer surface of HNTs is mostly occupied by Si-O-Si groups with a few Si-OH groups exposed on the edges of sheets or possible defects. [2] Therefore, the strong electronegativity of oxygen atoms makes the outer surface negatively charged. Meanwhile, the lower density of hydroxyl groups on the outermost surface along with

Environmental Science: Nano Accepted Manuscript

charged property endows HNTs with well dispersion ability in nonpolar polymers, offering enormous advantages for the preparation of HNTs/polymer nanocomposites. In addition, the abundant Al-OH groups in the inner surface with high activity facilitate the selective modification or immobilization of guest molecules in the lumen space. These surface groups can be confirmed by FTIR results as presented in Fig. 2d. The peaks at 3692.1 cm^{-1} and 3618.6 cm^{-1} are attributed to Al_2-OH stretching vibrations and peak of 911.7 cm^{-1} is ascribed to corresponding bending vibrations.[37] The very strong absorption peak at 1030.7 cm^{-1} is assigned to indicative stretching vibrations of Si-O-Si groups.[37] Additionally, HNTs are also considered as reinforcing and flame retardancy materials when in HNTs/polymer nanocomposites because of the high aspect ratio (length/diameter) and the barriers against heat and mass transport.[2]

3. HNTs-derived applications in removal of heavy metal ions

As mentioned above, the lumens of HNTs could be loaded with various active chemicals and the surfaces (both innermost and outermost surfaces) are readily to be non-covalently or covalently functionalized. HNTs have been considered as ideal alternatives for the preparation of adsorbents for kinds of heavy metal ions removal from wastewater, such as Cu (II), Pb (II), Cd (II), Zn (II), Cr (IV), and Co (II). The removal of hazardous heavy metals from aqueous media including drinking water, industrial or domestic wastewater, and soil solutions is of environmental importance to reduce the problem of water pollution and/or shortage worldwide. Generally, natural HNTs without any modification can remove heavy metal ions from aqueous

Environmental Science: Nano Accepted Manuscript

media through the mechanisms of physical and/or chemisorption, site geometry, metal speciation etc. However, in order to enhance the affinity and loading capacity for heavy metal ions, HNTs were often decorated with some interesting nanomaterials and/or functional groups to endow with extra mechanism of complexation. Table 1 summarizes HNTs-derived applications in removal of heavy metal ions from aqueous media. Because of the layer structure, natural HNTs were always intercalated with active molecules to improve the loading capacity and reusability. For example, Khelifa and coworkers developed intercalated HNTs with sodium acetate at various contact time and found that the most intercalated sample was more effective as adsorbent of Cu (II) from aqueous solutions with a removal capacity around 50 mg/g.[43] Subsequently, Khelifa and coworkers compared the variation of Cu (II) adsorption capacity for a series of intercalated HNTs with Na^{+}, $NH4^{+}$ and Pb^{2+} acetate, in which they believed that the Cu (II) adsorption capacity was not only related to intercalated fraction of acetate but also partly attributed to cations exchange on the negative surface sites.[44] Another approach to fabricating intercalated HNTs was proposed by Matusik et al. with diethanolamine and triethanolamine molecules as shown in Fig. 4.[45] The tailored HNTs adsorption capacity in terms of Pb (II), Cd (II), Zn (II), and Cu(II) was significantly improved due to a two-step gradual diffusion of the metals into the interlayer space and subsequent binding by amine nitrogen of the grafted aminoalcohol.

Besides the aforementioned studies on non-covalently modified HNTs, there are more emerging works on covalently functionalized HNTs. Chang et al. [46] reported

Environmental Science: Nano Accepted Manuscript

2-hydroxybenzoic acid (HBA) modified HNTs as a selective sorbent in solid phase exaction for separation and preconcentration of trance Fe (III) in aqueous media. The functionalized HNTs offered excellent selective solid phase exaction for Fe (III) with an enrichment factor of 75 and the maximum adsorption capacity was found to be 45.54 mg/g at optimum conditions. As solid phase exaction has become one of the most popular preconcentratio/separation methods, He et al. [48] also demonstrated acid-functionalized HNTs with N-2-Pyridylsuccinamic for solid phase exaction of Pb (II). In their work, an enrichment factor of 65 and the maximum adsorption capacity of 25.38 mg/g for Pb (II) were obtained. For the removal of Cr (VI) from aqueous solutions, Mishra and Maity et al. [49] fabricated a polypyrrole-coated HNTs nanocomposite via in situ polymerization of pyrrole onto HNTs. The authors announced a maximum adsorption capacity of 149.25 mg/g for Cr (VI) at pH 2.0 at 25^{o}C and the final nanocomposite was able to be reused three times without loss of its original removal efficiency. Apart from the adsorption capacity, the adsorption rate is another important factor for the evaluating of HNTs-based adsorbents. To increase the adsorption rate for Cr (VI), Zhang et al. [50] proposed a novel HNTs-based adsorbent modified with a surfactant of hexadecyltrimethylammonium bromide. The modified HNTs exhibited rapid adsorption rate for chromates and were capable of approaching to 90% of maximum adsorption capacity within 5 min. The effects of pH and ionic strength on the adsorption capacity were also investigated in their work and the modified HNTs were able to be recovered by eluents after adsorption of Cr (VI). Additionally, in another work, Zhang et al. prepared silane coupling agent grafted

Environmental Science: Nano Accepted Manuscript

HNTs for Cr (VI) and also studied the rapid adsorption properties.[51] Interestingly and particularly, a continuous fixed bed column for adsorption of Cu (II) was developed by Zhang et al. using HNTs/alginate hybrid beads, which is shown in Fig. 5.[52] At the optimized bed height, influent concentration and flow rate conditions, the hybrid beds showed excellent removal capacity of 74.13 mg/g for Cu (II) and regeneration properties with favorable stability.

In some other works, the removal properties of natural HNTs without any treatment for Zn,[53] Co,[54] Ag [55] were also systematically investigated. Compared to chemical method to remove heavy metal ions from aqueous solutions, HNTs-derived adsorbents showed great advantages such as lower cost, easily operating, reusability, non-secondary-pollution etc. Meanwhile, functionalized HNTs provided much higher removal capacity (6.611~149.25 mg/g) for heavy metal ions in marked contrast to natural HNTs (less than 10 mg/g), which is clearly displayed in Table 1.

4. HNTs-derived applications in removal of dyes

Dyes are extensively used in fields like paper, plastic, leather, cosmetic, textile and food industries, however, dye-contained wastewater in these industries have to be treated carefully before discharging. The dye-contained wastewater if discharged into natural streams may cause various serious environmental problems, such as disturbing the aquatic photosynthesis and damaging the ecosystem. Therefore, the removal of dyes from wastewater has received considerable attention over the past decades.[56-58] Similar with adsorption capacity for heavy metal ions, HNTs or HNTs-derived

Environmental Science: Nano Accepted Manuscript

composites also present superior removal capacity for dyes from dye-contaminated wastewater. Natural HNTs are capable of adsorbing both cationic and anionic dyes because of the negative Si-O-Si on the outermost surface and the positive Al-OH on the inner lumen surface (pH 4~9). Recently, a number of studies on removal of cationic-, neutral- and anionic-dyes from aqueous solution onto natural HNTs have been reported.[59-65] These works were based on the adsorption mechanisms including physical and chemisorption, site geometry etc. and showed moderate adsorption capacity (26~113.46 mg/g) and reusability.

Some other methods, HNTs were modified with Fe_3O_4 nanoparticles to combine magnetic separation technology with adsorption process for dyes removal from aqueous media.[66-68] Magnetically modified HNTs can be easier to separate from target aqueous solution after adsorption of dyes. Zhang and Liu et al. [67] developed a magnetic nanocomposite of Fe_3O_4-HNTs by a chemical precipitation method. The resulted adsorbent maintained a high adsorption capacity for methyl violet of 88.32 mg/g and also exhibited a fine magnetic property for the magnetic isolation. Liu and coworkers described a HNTs/Fe_3O_4/Carbon nanocomposite through an in-situ growth of Fe_3O_4 nanoparticles and a hydrothermal carbonization process of glucose on the surface of HNTs, which is shown in Fig. 6.[68] The authors declared that the as-prepared nanocomposite is a fast, separatable and superparamagnetic adsorbent with enhanced adsorption ability (57.13 mg/g), where the values for natural HNTs and HNTs/Fe3O4 were 38.73 mg/g, 29.33 mg/g, respectively, at the same optimized conditions. Generally, magnetically modified HNTs may lose some adsorption capacity to a

Environmental Science: Nano Accepted Manuscript

certain degree compared to the pristine HNTs as confirmed by the reported literatures. [66-68]

For strengthening the adsorption capacity, chitosan,[69] alginate,[70] graphene [71, 72] and the like have been adopted to construct HNTs-based adsorbents for the removal of dyes from aqueous media. Liu and Zhou et al. [69] prepared composite hydrogel beads containing chitosan and HNTs by a dropping and pH-precipitation method (as shown in Fig. 7). The composite hydrogel were employed to remove methylene blue and malachite green from aqueous solutions, exhibiting improved thermal stability and reinforced adsorption ability (72.60 mg/g for methylene blue and 276.9 mg/g for malachite green). Liu and Zhang et al. [71] described an HNTs@rGO composite (HGC) through homogeneous loading of HNTs on the surface of reduced graphene oxide sheets via an electrostatic self-assembly process (as shown in Fig. 8). The composite (HGC) showed a moderate adsorption capacity (45.4 mg/g) for rhodamine B (RhB) and high performance (23.6 F/g) as a supercapacitor. In another work, Zhang et al. [72] reported a spherical zeolite/reduced graphene oxide composite established via blending HNTs-derived zeolite with graphene oxide nanosheets (see Fig. 9). Although the tubular structure of HNTs was destroyed after hydrothermal reaction and regenerated cubic or spherical zeolite as described in their work, the synthesized composite still showed an adsorption capacity of 53.3 mg/g for methylene blue and a smaller value of 48.6 mg/g for malachite green.

Theoretically, the works mentioned above in applications for dyes removal are based

Environmental Science: Nano Accepted Manuscript

on the adsorption mechanism. However, some researchers also proposed TiO_2-, [73-76] ZnO-, [76] Ag- [77, 78] and CeO_2- [78] functionalized HNTs for the removal of dyes from aqueous media based on the dual-mechanism of adsorption and photodegradation. Zheng et al. [73] deposited anatase TiO_2 on the surface of HNTs for the adsorption and photodegradation of methylene blue. As expected, the HNTs/TiO_2 composite exhibited an efficient photocatalytic activity in the decomposition of methylene blue. At a calcination temperature of 300 ^oC, methylene blue was degraded to a degree of 81.6% after 4 h treatment of UV irradiation. Chuan and coworkers [74] also fabricated TiO_2 mounted HNTs composite by the hydrolysis of tetrabutyl titanate at room temperature and it was found that the resulted composite was capable of decreasing the concentration of methylene blue aqueous solution rapidly due to the synthetic action of adsorption and photodecomposition. The photodecomposition activity test showed almost 50% methylene blue decomposed in 6 h and most decomposed in 48 h. In addition, a carbon-doped TiO2/HNTs hybrid nanofiber with enhanced visible-light photocatalytic performance was described by Liu et al. (as shown in Fig. 10). [75] The visible-light photocatalytic efficiency of the nanofiber on the degradation of methyl blue was greatly reinforced with a moderate HNTs doping amount 8%, far greater than that of commercial anatase TiO_2. Yang et al. [76] reported a HNTs/MO/Carbon nanocomposite by the deposition of metal oxide (MO) nanoparticles (ZnO, TiO_2) onto carbon-coated HNTs for photodegradation of methylene blue (see Fig. 11). They investigated the carbon effect on the photocatalytic activity and the results indicated that graphitic carbon could improve the conductivity of HNTs and lead to a significant

Environmental Science: Nano Accepted Manuscript

improvement in photocatalytic properties (see Fig. 12). Du et al. [77] reported a type of HNTs supported Ag nanoparticles for photocatalytic decomposition of methylene blue using tea polyphenols as reductant (see Fig. 13), which exhibited good catalytic activity and high removal capacity to methylene blue. Within 60 min, nearly 90% of the MB had been decomposed photo-catalytically by the HNTs/AgNPs catalyst. Ni et al. [78] prepared HNTs supported hybrid CeO_2-AgBr nanocomposite by a microwave mediated method (see Fig. 14a). The synergistic effect of CeO_2 and AgBr greatly promoted the photocatalytic activity and the introduction of AgBr species was found to extend spectral response from UV to visible region (see Fig. 14b).

Overall, different with removal of heavy metals, there are two main mechanisms for removal of dyes from dyes-contained wastewater, namely, single-role of adsorption and dual-roles of adsorption and degradation. Generally, dual-roles mechanism is more efficient than single-role mechanism because of its sustainability. While regeneration is necessary for single-role based adsorbents after adsorption of dyes and the capacity is losing with circles.

5. HNTs-derived applications in membrane separation

HNTs have been proved to be capable of facilitating mechanical strength, thermal stability and separation properties of HNTs-contained polymer membranes. Various types of membrane including ultrafiltration (UF), nanofiltration (NF), forward osmosis (FO), reverse osmosis (RO), membrane reactor (MR), nanofiber and microfiber membranes etc. have been reported adopting HNTs as inorganic fillers to

Environmental Science: Nano Accepted Manuscript

endow with special functions (as summarized in Table 3).[79-95] For instance, natural HNTs were incorporated to UF,[79] FO (see Fig. 15),[92] RO[93] or nanofiber[95] membrane matrix to reinforce the mechanical strength and improve hydrophilicity. As reported, all the mentioned membranes exhibited improved water flux compared to HNTs-free membranes due to the interesting characteristics of natural HNTs. One important factor is the hydrophilicity of natural HNTs, which may result in an increase in solubilization and diffusion of water molecules into membrane matrix and then facilitating water permeability of membranes. In addition, the formation of voids at the interface of embedded HNTs and the presence of lumen of HNTs possibly provide more short pathways for permeation of water molecules. In some other works, natural HNTs were functionalized with Ag nanoparticles,[80, 82] Cu (II) ions,[81] N-halamine,[87] lysozyme[88] etc. to prepare antimicrobial hybrid ultrafiltration membranes as reported by Zhang et al. In these membranes, functionalized HNTs provided efficient antibacterial performance against both gram-negative (*E. coli*) and gram-positive (*S. aureus*) bacteria in water filtration process (see Fig. 17 and Fig. 18). The antimicrobial phenomenon is mainly based on a contact-destruction mechanism, where the HNTs supported antibacterial reagents appear on the membrane surface and/or pore wall of hybrid membranes. In order to improve the anti-protein-fouling properties, 2-methacryloyloxyethyl phosphorylcholine (MPC) (see Fig. 19)[85] and dextran[86] etc. grafted HNTs were also blended to polymer membrane matrix to prepare anti-protein-fouling membranes, which showed improved pure water flux and antifouling properties. The antifouling properties of hybrid membranes benefit from

Environmental Science: Nano Accepted Manuscript

the improvement of membrane surface hydrophilicity after the introduction of modified HNTs. For the applications of dyes/salts separation in aqueous media, Zhang and Liu et al. proposed charged "loose" nanofiltration membranes fabricated through introducing charged functionalized HNTs into membrane matrix.[89, 90] This type "loose" nanofiltration membrane was confirmed to maintain relatively higher dyes rejection meanwhile "near-zero" salts rejection as shown in Fig. 20. There membranes therefore may find potential applications for direct separation of dyes/salts from dye-containing wastewater. Ismail et al. [94] reported a type of photocatalytic membrane reactor by the incorporation of TiO_2 modified HNTs into PVDF membrane matrix. The obtained nanocomposite membrane played the roles of both degradation and separation for bilge water. In fact, many other types HNTs-containing films/membranes were reported in literatures in recent years. Here, however, only membranes used for water treatment were reviewed.

In summary, polymer membranes containing HNTs are generally endowed with relatively higher hydrophilicity, water flux, mechanical strength and thermal stability. Significant properties of membranes, particularly for water treatment, like antimicrobial, antifouling, ion-exchange, photocatalysis etc. can also be obtained by inducing functionalized HNTs, as shown in Table 3.

6. Other HNTs-derived applications for water treatment

Hereinbefore, we have discussed about the applications of HNTs-derived composites as adsorbents in heavy metal ions and dyes adsorption/degradation. In fact, due to the

Environmental Science: Nano Accepted Manuscript

tubular structure and multiple surface groups, HNTs have been gradually found many other applications for contaminant adsorption/degradation. As listed in Table 4, adsorption/degradation of tetracycline,[96-100] ammonium ions,[101-104] 2,4-dichlorophenoxyacetic acid,[105] chloroanilines,[106] phenol-based contaminant [107, 108] and 5-aminosalicylic acid [109] etc. by HNTs-based composites from aqueous solutions have been reported. Li et al. [96] proposed highly-controllable core-shell nanorods for selective recognition and rapid adsorption of tetracycline by the loading of Fe_3O_4 into lumen of HNTs and the imprinted polymerization at the surface. The tunable nanoshell thickness would affect the saturation adsorption capacity to tetracycline and the largest saturation adsorption capacity appeared at a thickness of 35 nm. Wang et al. [97] also reported a magnetic HNTs-based composite of HNTs/CoFe3O4 for the removal of tetracycline hydrochloride from aqueous solutions. The authors investigated the pH, temperature, initial concentrations and reaction time effect on the adsorption capacity for tetracycline hydrochloride. For degradation of tetracycline, TiO_2-, [98] CdS- [99, 100] etc. functionalized HNTs were always adopted to realize the photodegradation property. Conducting polymers, carbon or metal ions were frequently introduced to metal oxide functionalized HNTs to enhance the electrical conductivity for photocatalysis.

Considering the removal of ammonium ions from aqueous solutions, Zhang and coworkers developed a series of zeolite, such as NaA zeolite, [101, 103] zeolite X,[102] zeolite Y [104] from natural HNTs by a hydrothermal method. The tubular structure of HNTs changed to cubic or spherical forms with high crystallinity and uniform pore

Environmental Science: Nano Accepted Manuscript

channels after the hydrothermal reaction (see Fig. 21 and Fig. 22). The synthesized zeolite or hybrid beads showed higher adsorption capacity and fast adsorption rate for ammonium ions (NH_4^+) and the authors believed such low cost adsorbents could be utilized for effective and environmental-friendly removal of NH_4^+ pollutants from wastewater.

Phenol-based pesticides were widely used in agriculture and considered as one of the most important endocrine disrupting chemicals present in the environment. Some of them, for instance, nonylphenol compounds, are stable in water and exhibit aquatic toxicity and estrogenic activity even at very lower concentration. HNTs were also employed as basis material to prepare some special adsorbents for adsorption/degradation of phenol-based pollutants. Zhang and coworkers [107] synthesized a HNTs/chitosan hybrid nanotube through the assembly onto HNTs and then immobilized horseradish peroxidase (HRP) on the hybrid nanotubes for the degradation of phenol (see Fig. 23). The immobilized HRP did not undergo activity loss and meanwhile exhibited commendable removal efficiency for phenol from wastewater. Szczubialka et al. [108] prepared a hybrid photosensitizer by the incorporation of Rose Bengal (RB) into HNTs for the photodegradation of phenol-based pesticide. The photosensitizer was found to be efficient for singlet oxygen generation and combine adsorption ability with photocatalytic properties.

7. Conclusions and future prospects

In this review, we summarized the general structure and main properties of HNTs and

Environmental Science: Nano Accepted Manuscript

provided an overview of very recent researches toward HNTs-derived nanocomposites for water treatment. Increasing exiting applications have been discovered due to the interesting characteristics of HNTs such as nanoscale lumen, high aspect ratio, different internal and external surface chemistry, and abundant deposition. HNTs-derive applications in water treatment mainly focused on removal of heavy metal ions and dyes from aqueous media, preparation of all kinds of mixed matrix membranes. There are three main mechanisms involved in this review for water treatment:

(1) Adsorption-predominant. Removal of heavy metal ions, part of the dyes or some organic pollutants from polluted water resources is based on this adsorption-predominant mechanism. The adsorption process of HNTs-based materials is a complicated, which may include physi- and/or chemisorption, site geometry, metal speciation and complexation effect.

(2) Combination of adsorption and degradation. For some degradable dyes or organic pollutants removal from wastewater, both adsorption and degradation (mostly, photodegradation) effects are the critical factors for the removal efficiency. TiO_2, Ag, CdS, enzyme etc. chemicals were loaded onto the lumen or external surface of HNTs to endow with additional degradation properties. The dual-mechanism of both adsorption and degradation showed advantages than either single mechanism. Dual-mechanism is more efficiency for the removal of degradable pollutants and is promising for future applications.

Environmental Science: Nano Accepted Manuscript

(3) Interfacial interaction and reinforcement. For membrane preparation, natural HNTs or functionalized HNTs were selected as nanofillers to reinforce membrane performance, such as mechanical strength, thermal stability and permeation properties. In addition, the incorporated functional reagents on the surface of HNTs are capable of endowing hybrid membranes with novel properties, such as antifouling, antimicrobial, and catalytic performance etc.

Overall, HNTs are promising and cost-effective materials in the future for preparation of functional organic/inorganic nanocomposites. The significant progresses toward HNTs-derived applications in water treatment may provide more opportunities for recycling and purification of industrial or domestic wastewater. Future studies should pay more attention on the improvement of operability, regeneration and processing capacity in practical applications.

Acknowledgements

This work was financially sponsored by the National Natural Science Foundation of China (Nos. 21376225 and 21476215), and Excellent Youth Development Foundation of Zhengzhou University (No. 1421324066).

Environmental Science: Nano Accepted Manuscript

References

1. P. Berthier, *Ann. Chim. Phys*, 1826, **32**, 332-335.
2. M. Liu, Z. Jia, D. Jia and C. Zhou, *Prog. Polym. Sci.*, 2014, **39**, 1498-1525.
3. D. Fix, D. V. Andreeva, Y. M. Lvov, D. G. Shchukin and H. Möhwald, *Adv. Funct. Mater.*, 2009, **19**, 1720-1727.
4. H. Schmitt, N. Creton, K. Prashantha, J. Soulestin, M. Lacrampe and P. Krawczak, *Polym. Eng. Sci.*, **55**, 573-580.
5. S. A. Garea, A. Ghebaur and E. Vasile, *Mater. Plast.*, 2014, **51**, 124-129.
6. H. Wu, Y. Shi, C. Huang, Y. Zhang, J. Wu, H. Shen and N. Jia, *J. Biomater. Appl.*, 2014, **28**, 1180-1189.
7. P. áLo Meo, *J. Mat. Chem. B*, 2014, **2**, 7732-7738.
8. L. Fan, B. Li, Q. Wang, A. Wang and J. Zhang, *Adv. Mater. Interfaces*, 2014, **1**.
9. G. Cavallaro, G. Lazzara, S. Milioto, G. Palmisano and F. Parisi, *J. Colloid Interface Sci.*, 2014, **417**, 66-71.
10. N. G. Veerabadran, D. Mongayt, V. Torchilin, R. R. Price and Y. M. Lvov, *Macromol. Rapid Commun.*, 2009, **30**, 99-103.
11. Y. Suh, D. Kil, K. Chung, E. Abdullayev, Y. Lvov and D. Mongayt, *J. Nanosci. Nanotechnol.*, 2011, **11**, 661-665.
12. H. Kelly, P. Deasy, E. Ziaka and N. Claffey, *Int. J. Pharm.*, 2004, **274**, 167-183.
13. S. Feitosa, J. Palasuk, K. Kamocki, S. Geraldeli, R. Gregory, J. Platt, L. Windsor and M. Bottino, *J Dent. Res.*, 2014, **93**, 1270-1276.
14. A. D. Hughes and M. R. King, *Langmuir*, 2010, **26**, 12155-12164.
15. A. D. Hughes, J. Mattison, J. D. Powderly, B. T. Greene and M. R. King, *J. Vis. Exp.*, 2012, **64**, e4248.
16. M. Liu, L. Dai, H. Shi, S. Xiong and C. Zhou, *Mater. Sci. Eng. C-Biomimetic Supramol. Syst.*, 2015.
17. M. Liu, C. Wu, Y. Jiao, S. Xiong and C. Zhou, *J. Mat. Chem. B*, 2013, **1**, 2078-2089.
18. G. Nitya, G. T. Nair, U. Mony, K. P. Chennazhi and S. V. Nair, *J. Mater. Sci.: Mater. Med.*, 2012, **23**, 1749-1761.
19. W. Y. Zhou, B. Guo, M. Liu, R. Liao, A. B. M. Rabie and D. Jia, *J. Biomed. Mater. Res. Part A*, 2010, **93**, 1574-1587.
20. D. G. Shchukin, G. B. Sukhorukov, R. R. Price and Y. M. Lvov, *Small*, 2005, **1**, 510-513.
21. Y. Fu, L. Zhang and J. Zheng, *J. Nanosci. Nanotechnol.*, 2005, **5**, 558-564.
22. A. Wang, F. Kang, Z. Huang, Z. Guo and X. Chuan, *Microporous Mesoporous Mater.*, 2008, **108**, 318-324.
23. M. Du, B. Guo and D. Jia, *Polym. Int.*, 2010, **59**, 574-582.
24. Y. Lvov and E. Abdullayev, *Prog. Polym. Sci.*, 2013, **38**, 1690-1719.
25. J. Jiang, Y. Zhang, D. Cao and P. Jiang, *Chem. Eng. J.*, 2013, **215**, 222-226.
26. L. Yu, Y. Zhang, B. Zhang and J. Liu, *Scientific reports*, 2014, **4**.
27. H. Zhang, T. Zhang, J. Wang, F. Pei, Y. He and J. Liu, *Fuel Cells*, 2013, **13**,

Environmental Science: Nano Accepted Manuscript

1155-1165.
28. H. Bai, H. Zhang, Y. He, J. Liu, B. Zhang and J. Wang, *J. Membr. Sci.*, 2014, **454**, 220-232.
29. H. Zhang, C. Ma, J. Wang, X. Wang, H. Bai and J. Liu, *Int. J. Hydrogen Energy*, 2014, **39**, 974-986.
30. R. Zhai, B. Zhang, L. Liu, Y. Xie, H. Zhang and J. Liu, *Catal. Commun.*, 2010, **12**, 259-263.
31. L. Yan, J. Jiang, Y. Zhang and J. Liu, *J. Nanopart. Res.*, 2011, **13**, 6555-6561.
32. Y. Zhang, Y. Chen, H. Zhang, B. Zhang and J. Liu, *J. Inorg. Biochem.*, 2013, **118**, 59-64.
33. C. Liu, L. Yu, Y. Zhang, B. Zhang, J. Liu and H. Zhang, *RSC Adv.*, 2013, **3**, 13756-13763.
34. C. Chao, J. Liu, J. Wang, Y. Zhang, B. Zhang, Y. Zhang, X. Xiang and R. Chen, *ACS Appl. Mater. Interfaces*, 2013, **5**, 10559-10564.
35. X. Ding, H. Wang, W. Chen, J. Liu and Y. Zhang, *RSC Adv.*, 2014, **4**, 41993-41996.
36. A.-P. Wang, F. Kang, Z.-H. Huang and Z. Guo, *Clays Clay Miner.*, 2006, **54**, 485-490.
37. E. Joussein, S. Petit, J. Churchman, B. Theng, D. Righi and B. Delvaux, *Clay Miner.*, 2005, **40**, 383-426.
38. P. Pasbakhsh, G. J. Churchman and J. L. Keeling, *Appl. Clay Sci.*, 2013, **74**, 47-57.
39. U. A. Handge, K. Hedicke-Höchstötter and V. Altstädt, *Polymer*, 2010, **51**, 2690-2699.
40. A. Alhuthali and I. M. Low, *J. Mater. Sci.*, 2013, **48**, 4260-4273.
41. E. Abdullayev, A. Joshi, W. Wei, Y. Zhao and Y. Lvov, *ACS Nano*, 2012, **6**, 7216-7226.
42. F. Dong, J. Wang, Y. Wang and S. Ren, *J. Mater. Chem.*, 2012, **22**, 11093-11100.
43. S. Mellouk, A. Belhakem, K. Marouf-Khelifa, J. Schott and A. Khelifa, *J. Colloid Interface Sci.*, 2011, **360**, 716-724.
44. S. Mellouk, S. Cherifi, M. Sassi, K. Marouf-Khelifa, A. Bengueddach, J. Schott and A. Khelifa, *Appl. Clay Sci.*, 2009, **44**, 230-236.
45. J. Matusik and A. Wścisło, *Appl. Clay Sci.*, 2014, **100**, 50-59.
46. R. Li, Z. Hu, S. Zhang, Z. Li and X. Chang, *Int. J. Environ. Anal. Chem.*, 2013, **93**, 767-779.
47. R. Li, Q. He, Z. Hu, S. Zhang, L. Zhang and X. Chang, *Anal Chim Acta*, 2012, **713**, 136-144.
48. Q. He, D. Yang, X. Deng, Q. Wu, R. Li, Y. Zhai and L. Zhang, *Water Res.*, 2013, **47**, 3976-3983.
49. N. Ballav, H. J. Choi, S. B. Mishra and A. Maity, *Appl. Clay Sci.*, 2014, **102**, 60-70.
50. W. Jinhua, Z. Xiang, Z. Bing, Z. Yafei, Z. Rui, L. Jindun and C. Rongfeng, *Desalination*, 2010, **259**, 22-28.

Environmental Science: Nano Accepted Manuscript

51. P. Luo, J.-s. Zhang, B. Zhang, J.-h. Wang, Y.-f. Zhao and J.-d. Liu, *Ind. Eng. Chem. Res.*, 2011, **50**, 10246-10252.
52. Y. Wang, X. Zhang, Q. Wang, B. Zhang and J. Liu, *Water Sci. Technol.*, 2014, **70**, 192-199.
53. Y. Dong, Z. Liu and L. Chen, *J. Radioanal. Nucl. Chem.*, 2012, **292**, 435-443.
54. J. Li, F. Wen, L. Pan, Z. Liu and Y. Dong, *J. Radioanal. Nucl. Chem.*, 2013, **295**, 431-438.
55. G. Kiani, *Appl. Clay Sci.*, 2014, **90**, 159-164.
56. X. S. Wang, Y. Zhou, Y. Jiang and C. Sun, *J. Hazard. Mater.*, 2008, **157**, 374-385.
57. R. O. Cristóvão, A. P. Tavares, L. A. Ferreira, J. M. Loureiro, R. A. Boaventura and E. A. Macedo, *Bioresour Technol*, 2009, **100**, 1094-1099.
58. V. S. Mane, I. D. Mall and V. C. Srivastava, *Dyes Pigm.*, 2007, **73**, 269-278.
59. M. Zhao and P. Liu, *Microporous Mesoporous Mater.*, 2008, **112**, 419-424.
60. R. Liu, B. Zhang, D. Mei, H. Zhang and J. Liu, *Desalination*, 2011, **268**, 111-116.
61. G. Kiani, M. Dostali, A. Rostami and A. R. Khataee, *Appl. Clay Sci.*, 2011, **54**, 34-39.
62. Y. Zhao, E. Abdullayev, A. Vasiliev and Y. Lvov, *J. Colloid Interface Sci.*, 2013, **406**, 121-129.
63. H. Chen, J. Zhao, J. Wu and H. Yan, *RSC Adv.*, 2014, **4**, 15389-15393.
64. P. Luo, Y. Zhao, B. Zhang, J. Liu, Y. Yang and J. Liu, *Water Res.*, 2010, **44**, 1489-1497.
65. P. Luo, B. Zhang, Y. Zhao, J. Wang, H. Zhang and J. Liu, *Korean J. Chem. Eng.*, 2011, **28**, 800-807.
66. Y. Xie, D. Qian, D. Wu and X. Ma, *Chem. Eng. J.*, 2011, **168**, 959-963.
67. J. Duan, R. Liu, T. Chen, B. Zhang and J. Liu, *Desalination*, 2012, **293**, 46-52.
68. L. Jiang, C. Zhang, J. Wei, W. Tjiu, J. Pan, Y. Chen and T. Liu, *Chem. Res. Chin. Univ.*, 2014, **30**, 971-977.
69. Q. Peng, M. Liu, J. Zheng and C. Zhou, *Microporous Mesoporous Mater.*, 2015, **201**, 190-201.
70. L. Liu, Y. Wan, Y. Xie, R. Zhai, B. Zhang and J. Liu, *Chem. Eng. J.*, 2012, **187**, 210-216.
71. Y. Liu, X. Jiang, B. Li, X. Zhang, T. Liu, X. Yan, J. Ding, Q. Cai and J. Zhang, *J. Mater. Chem. A*, 2014, **2**, 4264-4269.
72. J. Zhu, Y. Wang, J. Liu and Y. Zhang, *Ind. Eng. Chem. Res.*, 2014, **53**, 13711-13717.
73. Y. Du and P. Zheng, *Korean J. Chem. Eng.*, 2014, **31**, 2051-2056.
74. L. Xianchu, C. Xiuyun, W. Aiping and K. Feiyu, *Acta Geologica Sinica (English Edition)*, 2006, **80**, 278-284.
75. L. Jiang, Y. Huang and T. Liu, *J. Colloid Interface Sci.*, 2015, **439**, 62-68.
76. Y. Zhang, J. Ouyang and H. Yang, *Appl. Clay Sci.*, 2014, **95**, 252-259.
77. M. Zou, M. Du, H. Zhu, C. Xu and Y. Fu, *J. Phys. D: Appl. Phys.*, 2012, **45**, 325302.

Environmental Science: Nano Accepted Manuscript

78. X. Li, C. Yao, X. Lu, Z. Hu, Y. Yin and C. Ni, *Appl. Clay Sci.*, 2015, **104**, 74-80.
79. J. Zhang, Y. Zhang, Y. Chen, S. Yi, B. Zhang, H. Zhang and J. Liu, *Adv. Sci. Lett.*, 2012, **11**, 57-62.
80. J. Zhang, Y. Zhang, Y. Chen, L. Du, B. Zhang, H. Zhang, J. Liu and K. Wang, *Ind. Eng. Chem. Res.*, 2012, **51**, 3081-3090.
81. Y. Chen, Y. Zhang, J. Liu, H. Zhang and K. Wang, *Chem. Eng. J.*, 2012, **210**, 298-308.
82. Y. Chen, Y. Zhang, H. Zhang, J. Liu and C. Song, *Chem. Eng. J.*, 2013, **228**, 12-20.
83. L. Duan, Q. Zhao, J. Liu and Y. Zhang, *Environmental Science: Water Research & Technology*, 2015, 1, 874-881.
84. Q. Zhao, J. Hou, J. Shen, J. Liu and Y. Zhang, *J. Mater. Chem. A*, 2015, **3**, 18696-18705.
85. Z. Wang, H. Wang, J. Liu and Y. Zhang, *Desalination*, 2014, **344**, 313-320.
86. H. Yu, Y. Zhang, X. Sun, J. Liu and H. Zhang, *Chem. Eng. J.*, 2014, **237**, 322-328.
87. L. Duan, W. Huang and Y. Zhang, *RSC Adv.*, 2015, **5**, 6666-6674.
88. Q. Zhao, C. Liu, J. Liu and Y. Zhang, *RSC Adv.*, 2015, **5**, 38646-38653.
89. J. Zhu, N. Guo, Y. Zhang, L. Yu and J. Liu, *J. Membr. Sci.*, 2014, **465**, 91-99.
90. L. Yu, Y. Zhang, H. Zhang and J. Liu, *Desalination*, 2015, **359**, 176-185.
91. Y. Wang, J. Zhu, G. Dong, Y. Zhang, N. Guo and J. Liu, *Sep. Purif. Technol.*, 2015, **150**, 243-251.
92. M. Ghanbari, D. Emadzadeh, W. Lau, S. Lai, T. Matsuura and A. Ismail, *Desalination*, 2015, **358**, 33-41.
93. M. Ghanbari, D. Emadzadeh, W. Lau, T. Matsuura and A. Ismail, *RSC Adv.*, 2015, **5**, 21268-21276.
94. A. Moslehyani, A. Ismail, M. Othman and T. Matsuura, *RSC Adv.*, 2015, **5**, 14147-14155.
95. M. Makaremi, R. T. De Silva and P. Pasbakhsh, *The Journal of Physical Chemistry C*, 2015, **119**, 7949-7958.
96. J. Dai, X. Wei, Z. Cao, Z. Zhou, P. Yu, J. Pan, T. Zou, C. Li and Y. Yan, *RSC Adv.*, 2014, **4**, 7967-7978.
97. W. Guan, X. Wang, J. Pan, J. Lei, Y. Zhou, C. Lu and Y. Yan, *Adsorpt. Sci. Technol.*, 2012, **30**, 579-592.
98. X. Yu, Z. Lu, N. Si, W. Zhou, T. Chen, X. Gao, M. Song, Y. Yan, P. Huo and C. Yan, *Appl. Clay Sci.*, 2014, **99**, 125-130.
99. W. Xing, L. Ni, X. Liu, Y. Luo, Z. Lu, Y. Yan and P. Huo, *RSC Adv.*, 2013, **3**, 26334-26342.
100. W. Xing, L. Ni, X. Liu, Y. Luo, Z. Lu, Y. Yan and P. Huo, *Desalination and Water Treatment*, 2015, **53**, 794-805.
101. Y. Zhao, B. Zhang, X. Zhang, J. Wang, J. Liu and R. Chen, *J. Hazard. Mater.*, 2010, **178**, 658-664.
102. Y. Zhao, B. Zhang, X. Zhang, J. Wang, J. Liu and R. Chen, *Water Sci. Technol.*

Environmental Science: Nano Accepted Manuscript

2010, **62**, 937-946
103. K. Yang, X. Zhang, C. Chao, B. Zhang and J. Liu, *Carbohydr. Polym.*, 2014, **107**, 103-109.
104. Y. Zhao, B. Zhang, Y. Zhang, J. Wang, J. Liu and R. Chen, *Sep. Sci. Technol.*, 2010, **45**, 1066-1075.
105. S. Zhong, C. Zhou, X. Zhang, H. Zhou, H. Li, X. Zhu and Y. Wang, *J. Hazard. Mater.*, 2014, **276**, 58-65.
106. B. Szczepanik, P. Słomkiewicz, M. Garnuszek and K. Czech, *Appl. Clay Sci.*, 2014, **101**, 260-264.
107. R. Zhai, B. Zhang, Y. Wan, C. Li, J. Wang and J. Liu, *Chem. Eng. J.*, 2013, **214**, 304-309.
108. D. Bielska, A. Karewicz, T. Lachowicz, K. Berent, K. Szczubiałka and M. Nowakowska, *Chem. Eng. J.*, 2015, **262**, 125-132.
109. M. Viseras, C. Aguzzi, P. Cerezo, C. Viseras and C. Valenzuela, *Microporous Mesoporous Mater.*, 2008, **108**, 112-116.

Environmental Science: Nano Accepted Manuscript

Table Captions

Table 1 HNTs-derived application in removal of heavy metals ions from aqueous media

Table 2 HNTs-derived application in removal of dyes from aqueous media

Table 3 HNTs-derived application in membrane separation

Table 4 Other HNTs-derived application for water treatment

Figure Captions

Fig. 1 Annual number of scientific publications based on the word "halloysite" for the last decade (Data analysis was done at 7th May, 2015)

Fig. 2 (a) TEM image, (b) crystalline structure, (c) XRD pattern and (d) FTIR curve of HNTs

Fig. 3 (a) Illustration of acid etching of alumina inner layers from HNTs lumen and (b) histogram of lumen and outer diameters for original and alumina etched HNTs [41]

Fig. 4 Approximate structure model of (a) triethanolamine and (b) diethanolamine intercalated HNTs [45]

Fig. 5 The schematic of HNTs/alginate fixed bed column for Cu (II) adsorption [52]

Fig. 6 Schematic showing of synthesis of HNTs/Fe_3O_4 /carbon nanocomposite [68]

Fig. 7 appearance of chitosan and HNTs-chitosan hydrogel beds in wet and dry state [69]

Fig. 8 (a) Construction process of HGC and (b) Uv-vis spectra of RhB solution and those after treatment with HGC at different times [71]

Fig. 9 Schematic showing of synthesis of zeolite/rGO composite [72]

Environmental Science: Nano Accepted Manuscript

Fig. 10 Schematic illustration of the synthesis of carbon-doped TiO2/HNTs hybrid nanofibers [75]

Fig. 11 Schematic of the fabrication for HNTs/MO/Carbon nanocomposite [76]

Fig. 12 Proposed mechanisms for enhanced photocatalytic activity of HNTs/MO/Carbon nanocomposite [77]

Fig. 13 Illustration of synthesis of HNTs supported AgNPs [77]

Fig. 14 (a) Scheme of photocatalytic degradation mechanism of HNTs/CeO2/AgBr nanocomposite and (b) photocatalytic degradation of methyl orange in aqueous solar light irradiation [78]

Fig. 15 Schematic diagram of HNTs/PA thin film composite forward osmosis membrane using PSf substrate [92]

Fig. 16 Reaction principle of HNTs-AgNPs for fabrication of antimicrobial membrane [80]

Fig. 17 Photographs showing the bacterial culture plates of (a) *E. coli* and (b) *S. aureus* to PES and PES/HNTs-AgNPs membranes [80]

Fig. 18 (a) SEM images of E. coli attached to PES membrane and N-halamine@HNTs/PES membrane; (b) Bacteriostasis rate measurement of PES membrane and N-halamine@HNTs/PES membrane [87]

Fig. 19 Schematic diagram of HNTs-MPC/PES anti-protein-fouling ultrafiltration membrane [85]

Fig.20 (a) Schematic showing fabrication process of HNTs-PIL/PES positively charged nanofiltration membrane and (b) rejections for dyes and salts of

Environmental Science: Nano Accepted Manuscript

HNTs-PIL/PES membranes as a function of HNTs-PIL content [90]

Fig. 21 XRD patterns of (a) zeolite X, (b) NaA zeolite, (c) zeolite Y and (d)SEM image of NaA zeolite synthesized from natural HNTs [101-104]

Fig. 22 Schematic showing the fabrication process of NaA zeolite/chitosan hybrid beads [103]

Fig. 23 Schematic illustration of (a) preparation of chitosan-halloysite hybrid nanotubes and (b) immobilization of horseradish peroxidase [107]

Environmental Science: Nano Accepted Manuscript

Table 1 HNTs-derived application in removal of heavy metals ions from aqueous media

Materials	Heavy metals	Feed conditions [1]	Removal capacity (mg/g)	Ref.
HNTs/CH_3COO^-	Cu (II)	10~200 mg/L; pH, 6	~50	43
HNTs/CH_3COONa	Cu (II)	10~200 mg/L; pH, 6	52.3	44
HNTs/aminoalcohols	Pb (II), Cd (II), Zn (II), Cu (II)	0.005~5.0 mmol/L; pH, 2.0~6.5	--	45
HNTs/HBA [2]	Fe (III)	10 mg/L; pH, 4	45.54	46
HNTs/murexide	Pd (II)	1mg/L; pH, 1~7	42.86	47
HNTs/PSA [3]	Pb (II)	1mg/mL; pH, 1~7	23.58	48
HNTs/PPy [4]	Cr (VI)	1000 mg/L; pH, 2~11	149.25	49
HNTs/HDTMA[5]	Cr (VI)	25~300 mg/L; pH, 3~10	6.611	50
HNTs/KH-792 [6]	Cr (VI)	0~400 mg/L; pH, 2~9	37.25	51
HNTs/alginate	Cu (II)	50~100 mg/L	74.13	52
Natural HNTs	Zn (II)	10 mg/L; pH, 2~9	9.87	53
Natural HNTs	Co (II)	10 mg/L; pH, 3~11	~6	54
Natural HNTs	Ag (I)	~50 mg/L	3~6	55

[1] Feed conditions demonstrates the initial concentration and pH of test heavy metal ions aqueous solution

[2] HBA represents the abbreviation of 2-hydroxybenzoic acid

[3] PSA represents the abbreviation of N-2-Pyridylsuccinamic acid

[4] PPy represents the abbreviation of polypyrrole

[5] HDTMA represents the abbreviation of hexadecyltrimethylammonium bromide

[6] KH-792 represents the abbreviation of N-β-aminoethyl-γ-aminopropyl trimethoxysilane

Environmental Science: Nano Accepted Manuscript

Table 2 HNTs-derived application in removal of dyes from aqueous media

Materials	Dyes	Mechanism	Feed concentration (mg/L) [1]	Removal capacity (mg/g)	Ref.
Natural HNTs	Methylene blue	Adsorption	100~300	84.32	59
Natural HNTs	Methyl violet	Adsorption	50~400	113.64	60
Natural HNTs	Malachite green	Adsorption	20~100	99.6	61
Natural HNTs	Rhodamine 6G & chrome azurol	Adsorption	300	43.6, 38.7	62
Natural HNTs	Methyl orange & Congo red	Adsorption	300	~26	63
Natural HNTs	Neutral red	Adsorption	50~400	65.45	64
Activated HNTs	Methylene blue	Adsorption	50~500	103.63	65
HNTs/Fe_3O_4	Methylene blue & neutral red & methyl orange	Adsorption	0.1 mmol/L	18.44	66
HNTs/Fe_3O_4	Methyl violet	Adsorption	50~400	88.2	67
HNTs/Fe_3O_4/Carbon	Methylene blue	Adsorption	10~70	57.13	68
HNTs/chitosan	Methylene blue & malachite green	Adsorption	20~400	72.60, 276.9	69
HNTs/alginate	Methylene blue	Adsorption	50~500	250	70
HNTs/rGO [2]	Rhodamine B	Adsorption	0.01 mmol/L	45.4	71
Zeolite/rGO [3]	Methylene blue & malachite green	Adsorption	50~300	53.3, 48.6	72
HNTs/TiO_2	Methylene blue	Adsorption & degradation	0.1 mmol/L	52.49	73
HNTs/TiO_2	Methylene blue	Adsorption &degradation	40	29.64	74
HNTs/TiO_2/Carbon	Methyl blue	Degradation	20	--	75
HNTs/MO/Carbon	Methylene blue	Adsorption &degradation	5	~50	76
HNTs/AgNPs [4]	Methyl blue	Degradation	0.0267 mmol/L	--	77
HNTs/CeO_2/AgBr	Methyl orange	Degradation	20	--	78

[1] Feed concentration demonstrates the initial concentration of test dyes aqueous solution, which is not the optimized concentration.

[2] rGO represents the abbreviation of reduced graphene oxide nanosheets

[3] Zeolite here was fabricated from natural HNTs by hydrothermal reaction.

[4] AgNPs represents the abbreviation of silver nanoparticles

Environmental Science: Nano Accepted Manuscript

Table 3 HNTs-derived application in membrane separation

Materials	Matrix	Membrane process or type	Function [1]	Ref.
Natural HNTs	PES [2]	UF [3]	Hydrophilic modification	79
HNTs/AgNPs	PES	UF	Antimicrobial	80
HNTs/Cu(II)	PES	UF	Antimicrobial	81
HNTs/Cs/AgNPs	PES	UF	Antimicrobial	82
HNTs/CuNPs [4]	PES	UF	Antimicrobial	83
HNTs/rGO/AgNPs	PES	UF	antimicrobial	84
HNTs/MPC [5]	PES	UF	Antifouling	85
HNTs/dextran	PES	UF	Antifouling	86
HNTs/N-halamine	PES	UF	Antimicrobial	87
HNTs/lysozyme	PES	UF	Antimicrobial	88
HNTs/PSS [6]	PES	NF [7]	Ion-exchange	89
HNTs/PIL [8]	PES	NF	Ion-exchange	90
Sulfonated HNTs	PES	NF	Ion-exchange	91
Natural HNTs	PA [9]	FO [10]	Antifouling	92
Natural HNTs	PA	RO [11]	Antifouling	93
HNTs/TiO_2	PVDF [12]	MR [13]	Photocatalyst	94
Natural HNTs	PAN [14]	Nanofiber	Reinforcement	95

[1] Function demonstrates the key role of HNTs-based materials play in membrane matrix

[2] PES represents the abbreviation of polyether sulfone

[3] UF represents the abbreviation of ultrafiltration

[4] CuNPs represents the abbreviation of copper nanoparticles

[5] MPC represents the abbreviation of 2-methacryloyloxyethyl phosphorylcholine

[6] PSS represents the abbreviation of poly (sodium 4-styrenesulfonate)

[7] NF represents the abbreviation of nanofiltration

[8] PIL represents the abbreviation of poly (ionic liquid)

[9] PA represents the abbreviation of polyamide

[10] FO represents the abbreviation of forward osmosis

[11] RO represents the abbreviation of reverse osmosis

[12]PVDF represents the abbreviation of polyvinylidene fluoride

[13] MR represents the abbreviation of membrane reactor

[14] PAN represents the abbreviation of polyacrylonitrile

Environmental Science: Nano Accepted Manuscript

Table 4 Other HNTs-derived application for water treatment

Materials	Applications	Ref.
HNTs/Fe_3O_4/MIP [1]	Adsorption of tetracycline	96
HNTs/$CoFe_2O_4$	Adsorption of tetracycline hydrochloride	97
HNTs/TiO_2/M^{n+}	Degradation of tetracycline	98
HNTs/CdS/PNIPAm [2]	Degradation of tetracycline	99
HNTs/CdS-M^{n+}	Degradation of tetracycline	100
NaA zeolite [3]	Adsorption of ammonium	101
Zeolite X [3]	Adsorption of ammonium	102
NaA zeolite/Chitosan [3]	Adsorption of ammonium	103
Zeolite Y [3]	Adsorption of ammonium	104
HNTs/Fe_3O_4/MIP	Enrichment of 2,4-dichlorophenoxyacetic acid	105
Acid-activated HNTs	Adsorption of chloroanilines	106
HNTs-CTS-GTA-HRP [4]	Degradation of phenol	107
HNTs/RB [5]	Degradation of phenol-based pesticide	108
Natural HNTs	Adsorption of 5-aminosalicylic acid	109

[1]MIP represents the abbreviation of molecularly imprinted polymer

[2] PNIPAM represents the abbreviation of poly (N-isopropylacrylamide)

[3]Zeolite was synthesized from natural HNTs by hydrothermal reaction

[4] CTS, GTA, HRP represent the abbreviations of chitosan, glutaraldehyde, and horseradish peroxidase, respectively

[5] RB represents the abbreviation of Rose Bengal

Environmental Science: Nano Accepted Manuscript

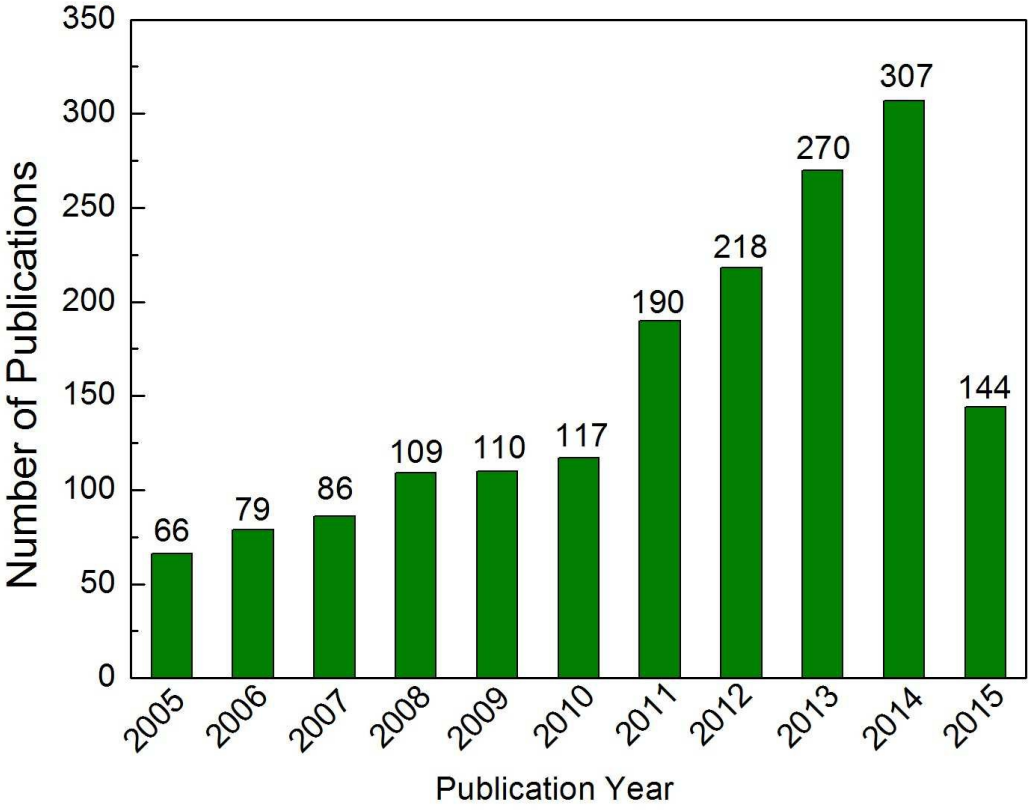

Fig. 1 Annual number of scientific publications based on the word "halloysite" for the last decade (Data analysis was done at 7th May, 2015)

Environmental Science: Nano Accepted Manuscript

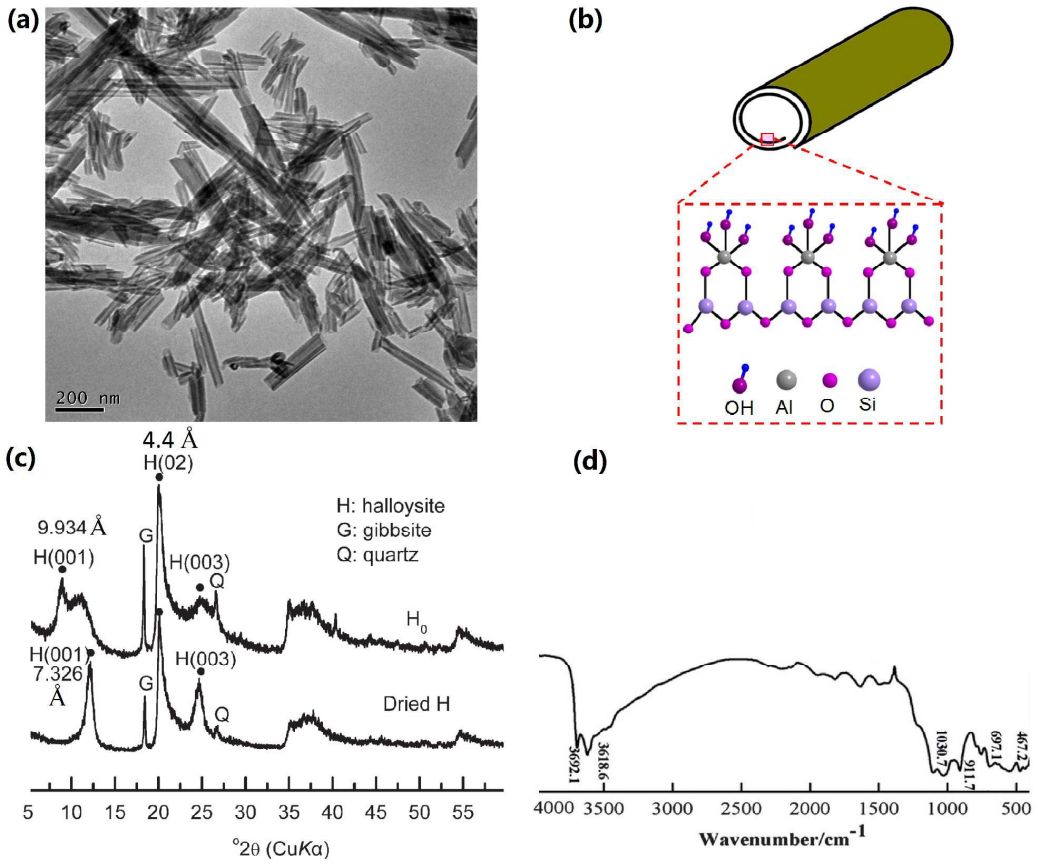

Fig. 2 (a) TEM image, (b) crystalline structure, (c) XRD pattern [36] and (d) FTIR curve [42] of natural HNTs.

Environmental Science: Nano Accepted Manuscript

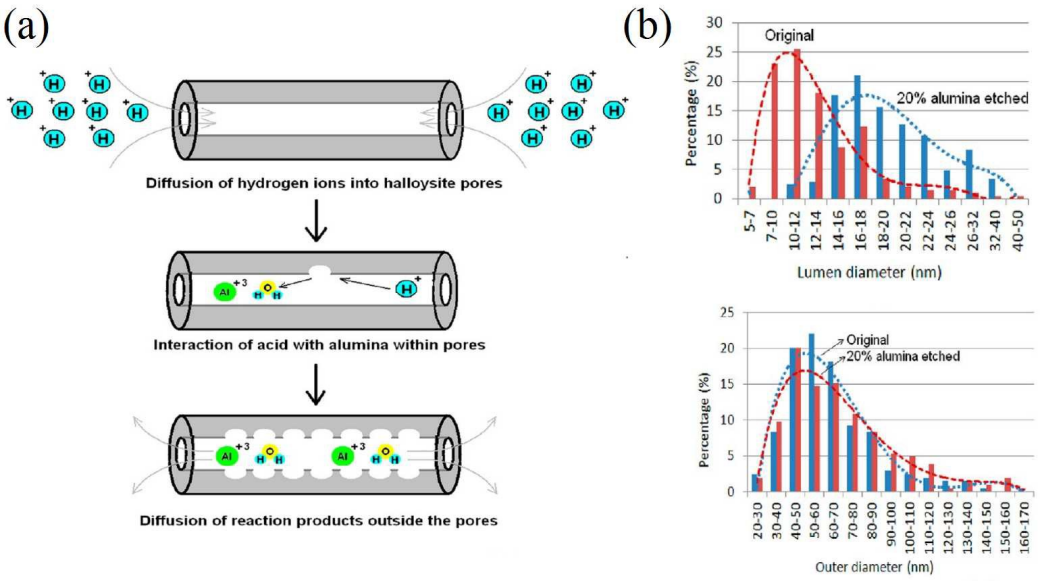

Fig. 3 (a) Illustration of acid etching of alumina inner layers from HNTs lumen and (b) histogram of lumen and outer diameters for original and alumina etched HNTs [41].

Environmental Science: Nano Accepted Manuscript

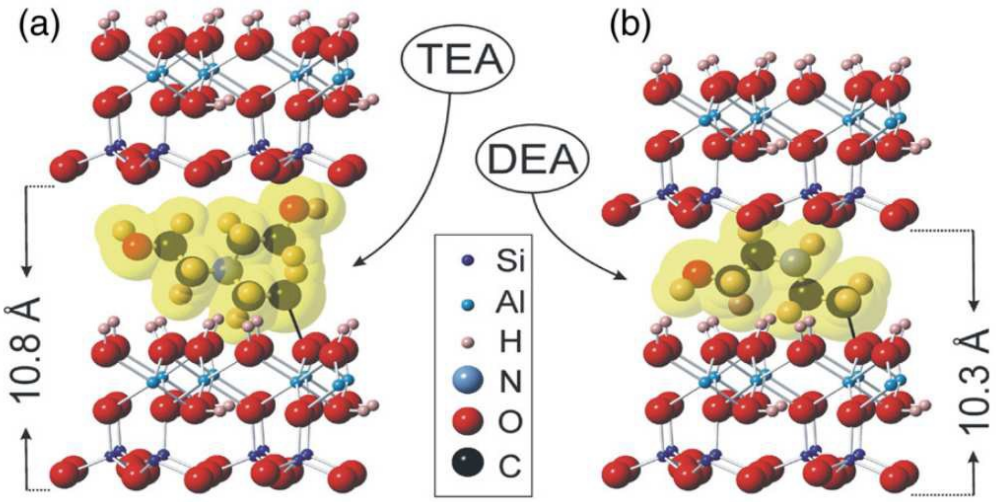

Fig. 4 Approximate structure model of (a) triethanolamine and (b) diethanolamine intercalated HNTs[45]

Environmental Science: Nano Accepted Manuscript

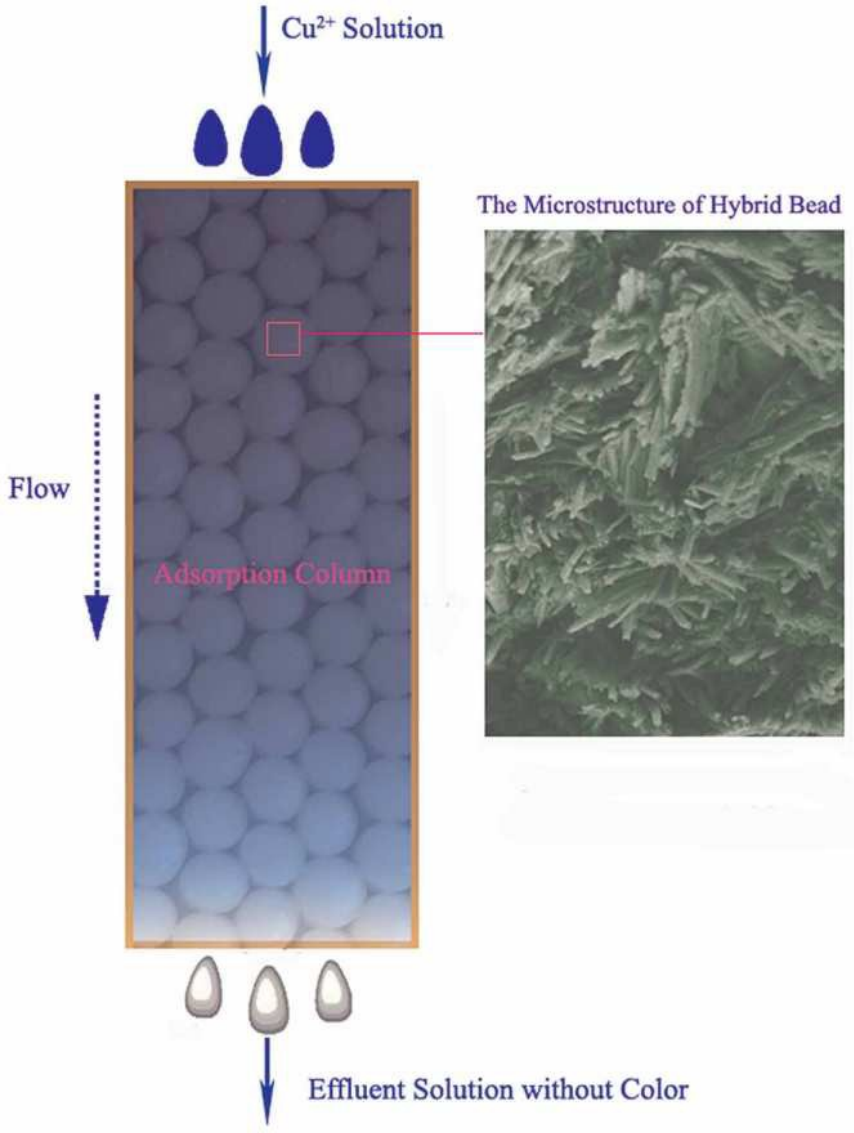

Fig. 5 The schematic of HNTs/alginate fixed bed column for Cu (II) adsorption [52]

Environmental Science: Nano Accepted Manuscript

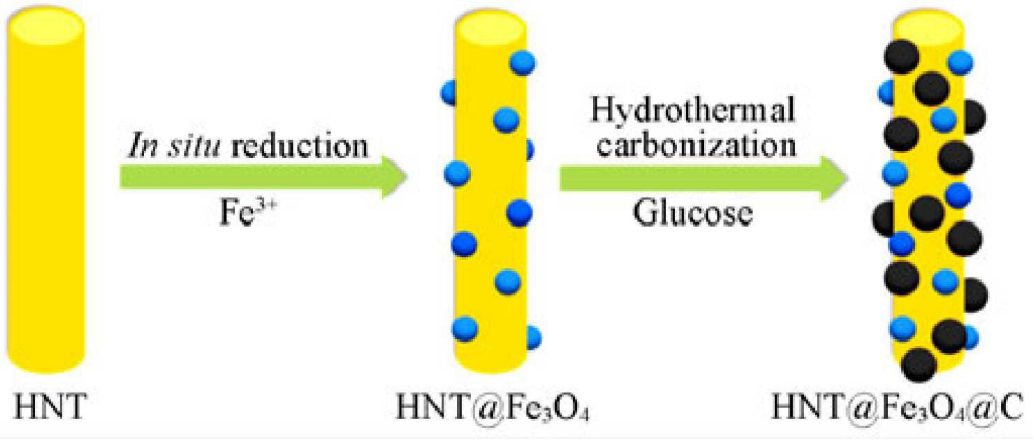

Fig. 6 Schematic showing of synthesis of HNTs/Fe_3O_4/carbon nanocomposite [68]

Environmental Science: Nano Accepted Manuscript

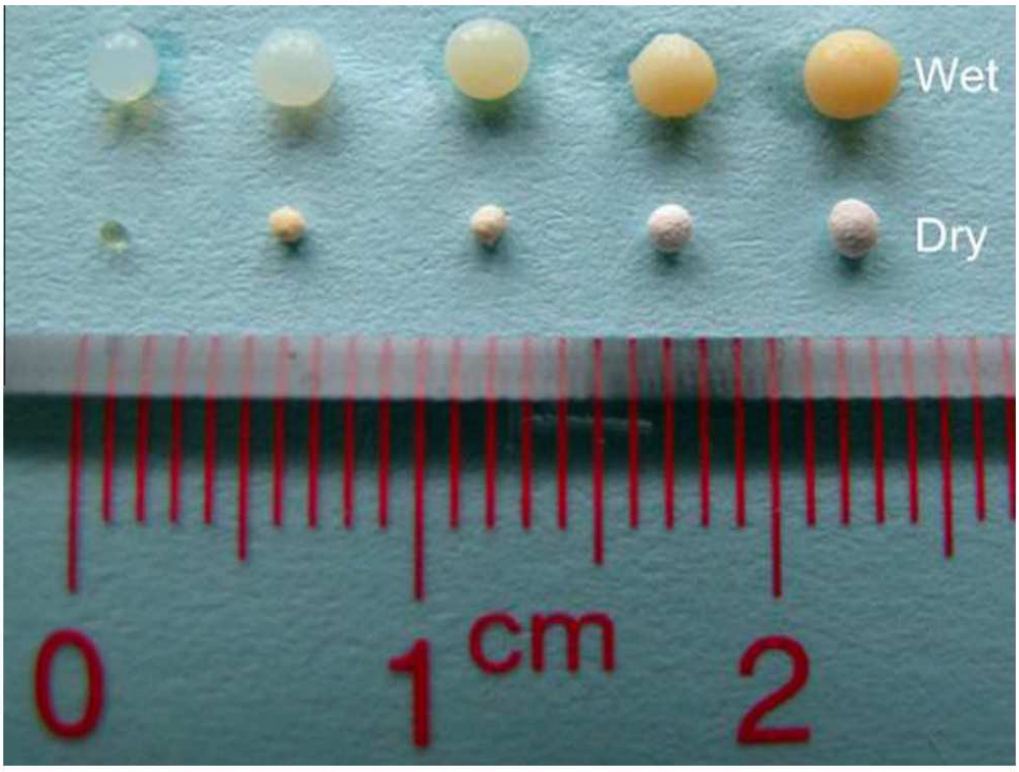

Fig. 7 Appearance of chitosan and HNTs-chitosan hydrogel beds in wet and dry state [69]

Environmental Science: Nano Accepted Manuscript

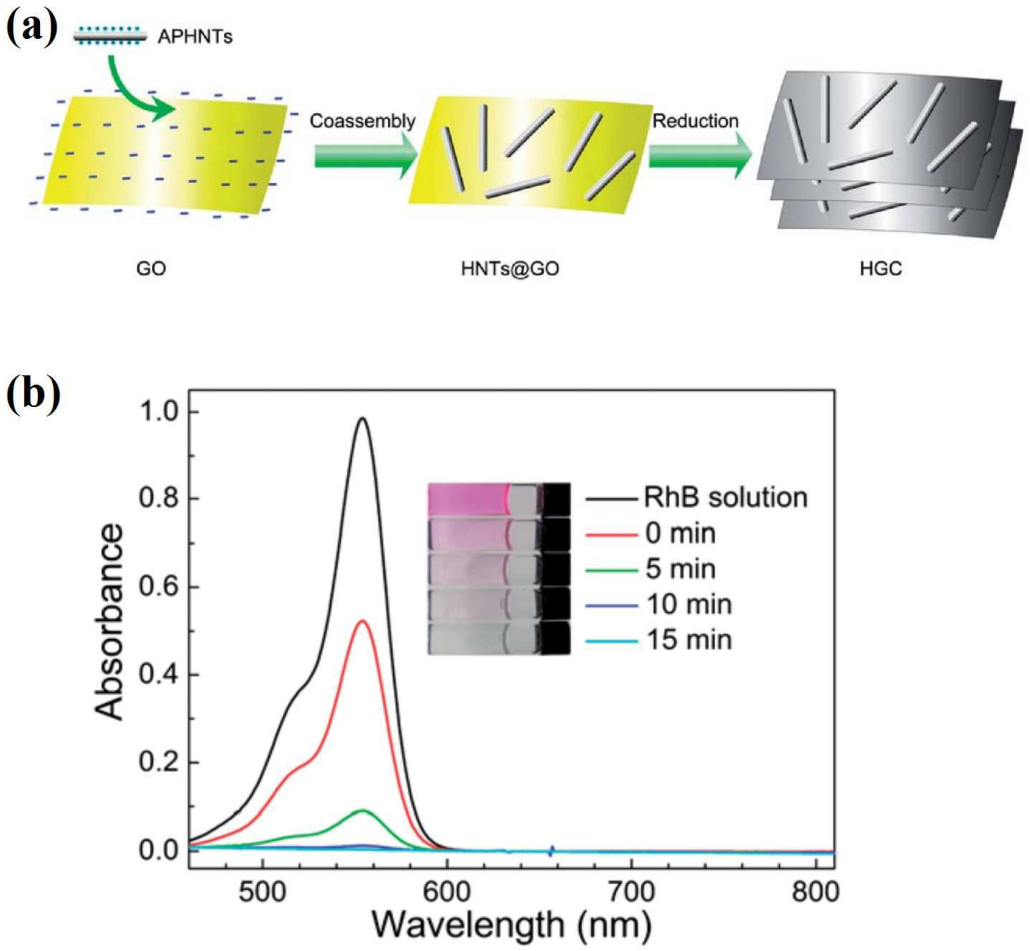

Fig. 8 (a) Construction process of HGC and (b) Uv-vis spectra of RhB solution and those after treatment with HGC at different times [71]

Environmental Science: Nano Accepted Manuscript

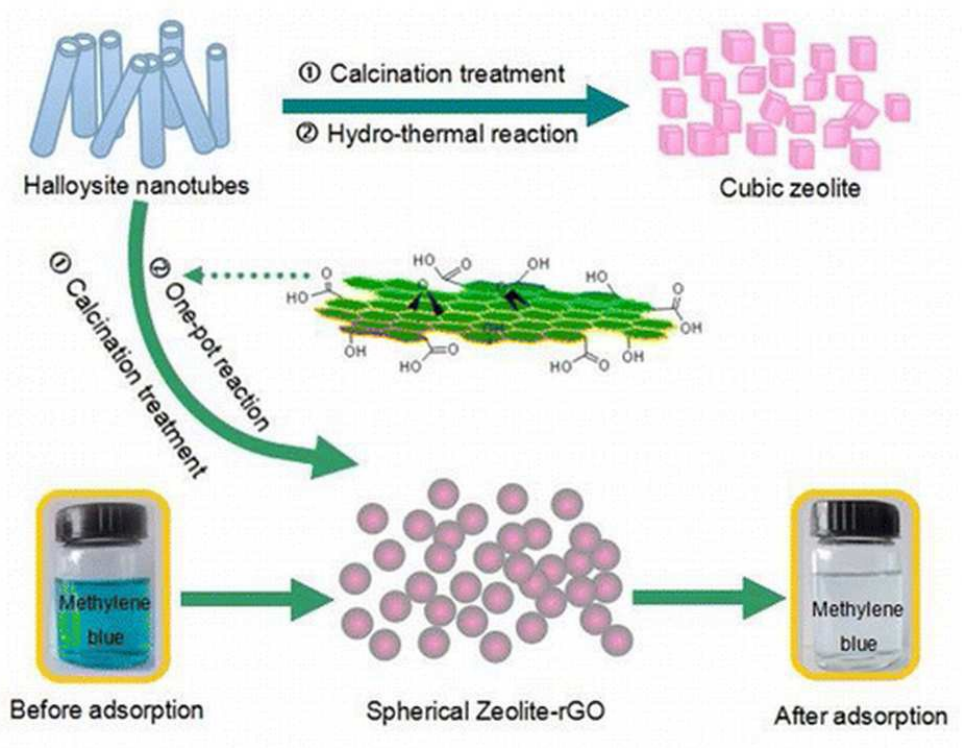

Fig. 9 Schematic showing of synthesis of zeolite/rGO composite [72]

Environmental Science: Nano Accepted Manuscript

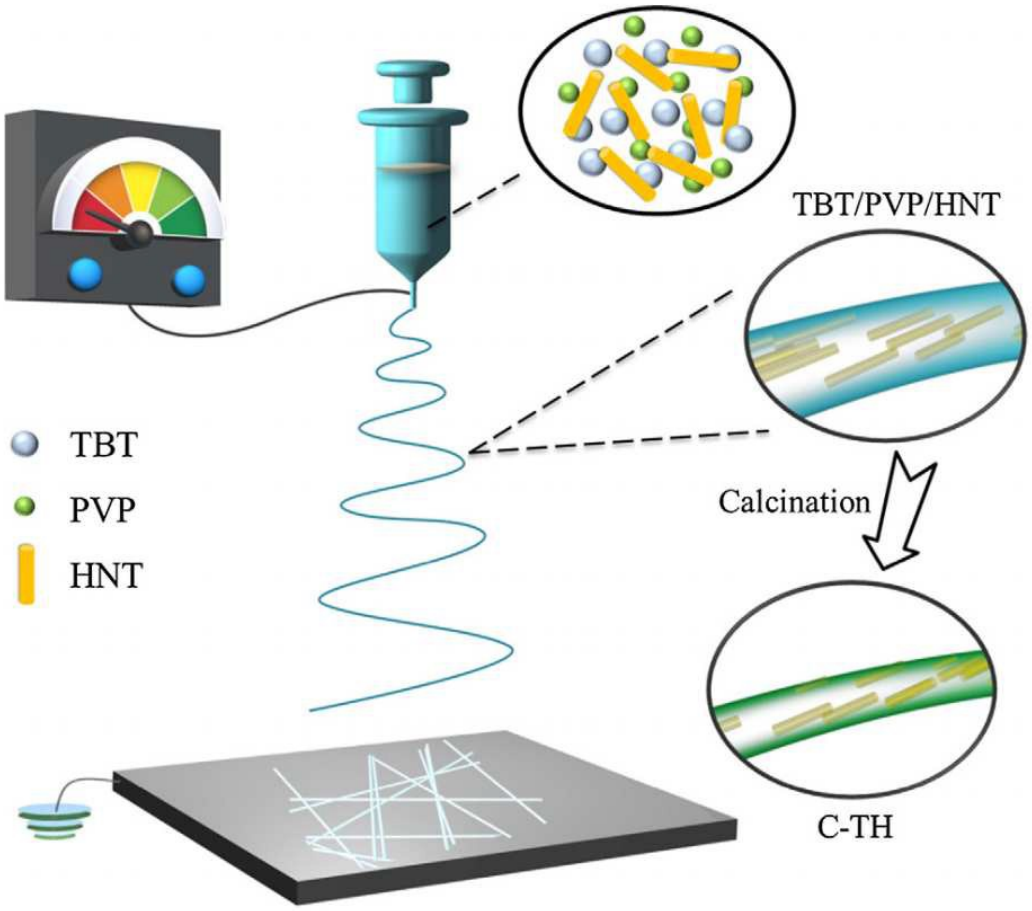

Fig. 10 Schematic illustration of the synthesis of carbon-doped TiO2/HNTs hybrid nanofibers [75]

Environmental Science: Nano Accepted Manuscript

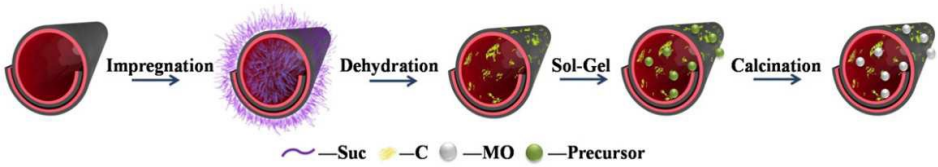

Fig. 11 Schematic of the fabrication for HNTs/MO/Carbon nanocomposite [76]

Environmental Science: Nano Accepted Manuscript

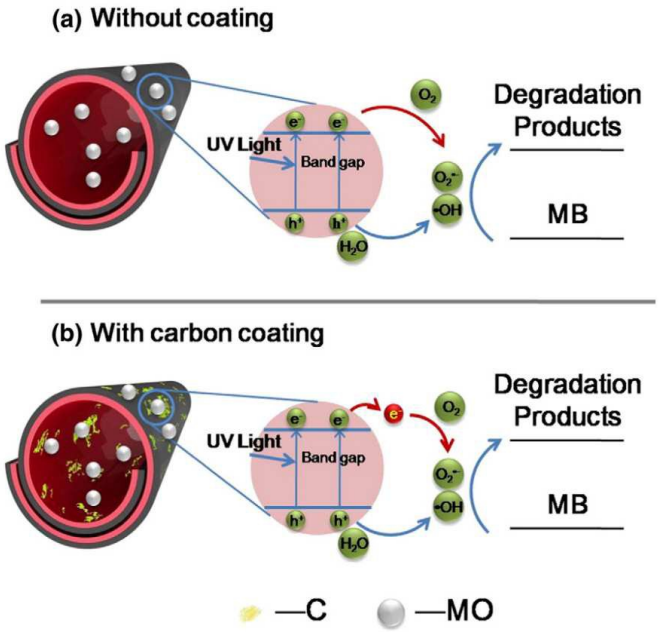

Fig. 12 Proposed mechanisms for enhanced photocatalytic activity of HNTs/MO/Carbon nanocomposite [77]

Environmental Science: Nano Accepted Manuscript

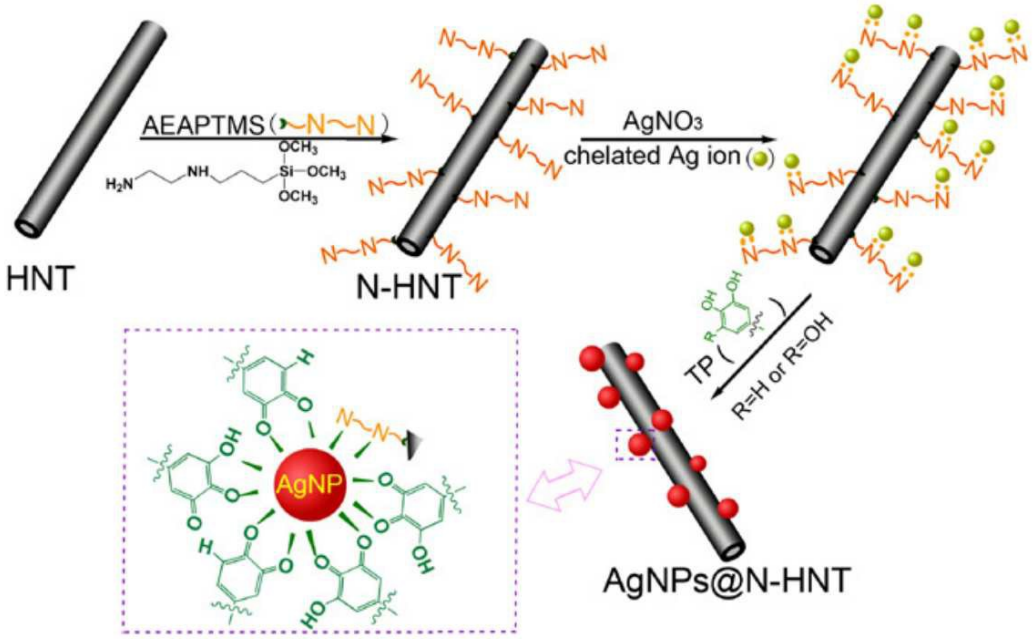

Fig. 13 Illustration of synthesis of HNTs supported AgNPs [77]

Environmental Science: Nano Accepted Manuscript

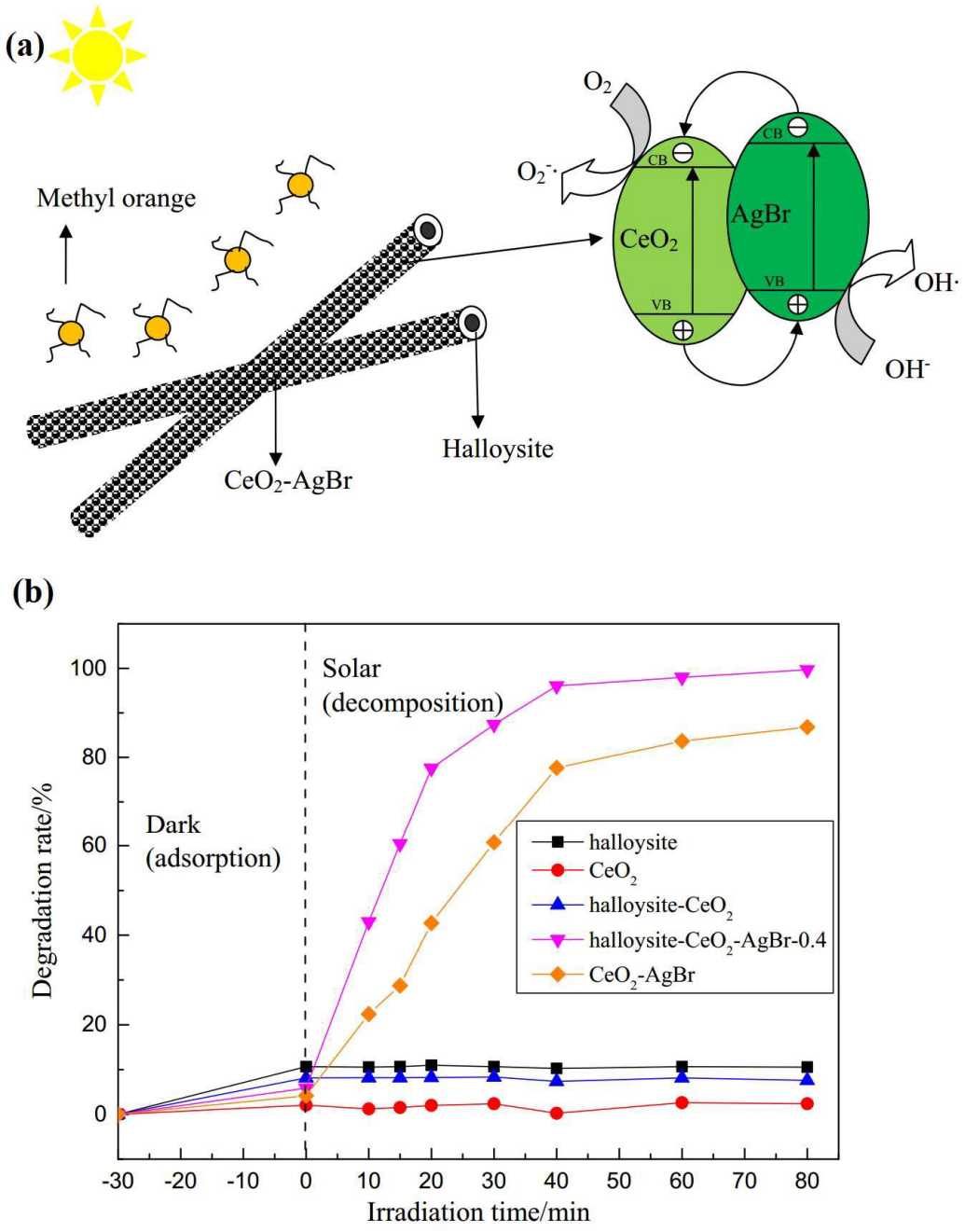

Fig. 14 (a) Scheme of photocatalytic degradation mechanism of HNTs/CeO_2/AgBr nanocomposite and (b) photocatalytic degradation of methyl orange in aqueous solar light irradiation [78]

Environmental Science: Nano Accepted Manuscript

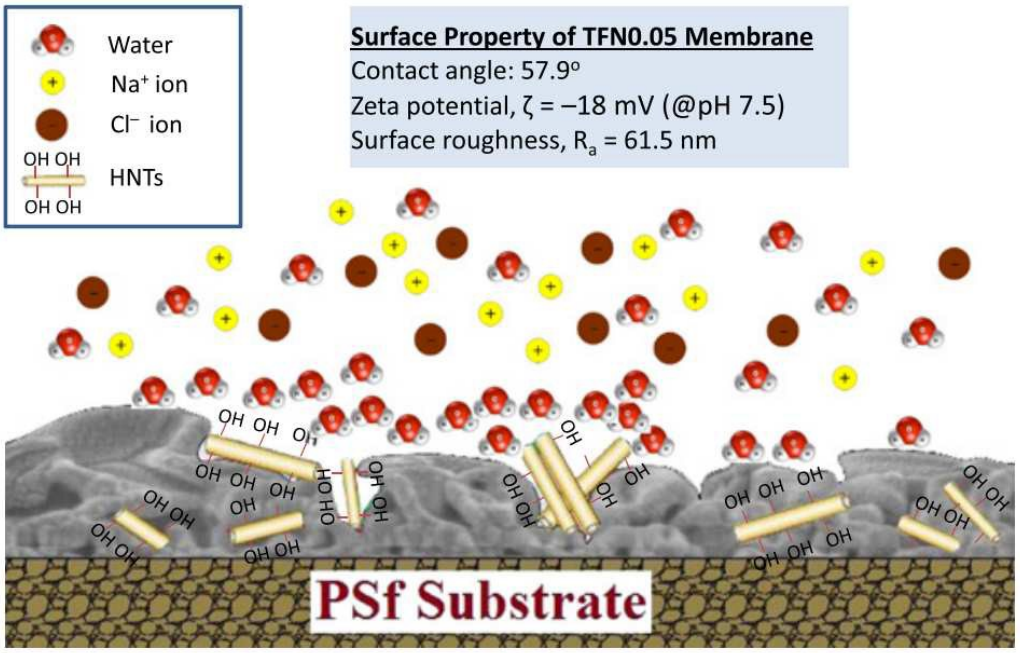

Fig. 15 Schematic diagram of HNTs/PA thin film composite forward osmosis membrane using PSf substrate [92]

Environmental Science: Nano Accepted Manuscript

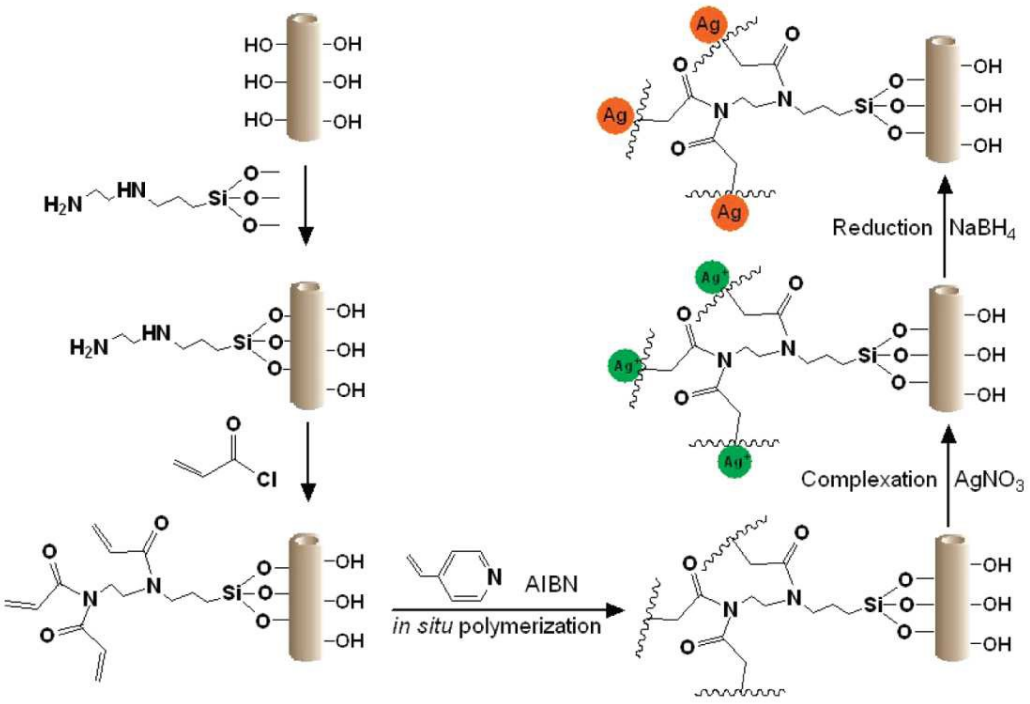

Fig. 16 Reaction principle of HNTs-AgNPs for fabrication of antimicrobial membrane [80]

Environmental Science: Nano Accepted Manuscript

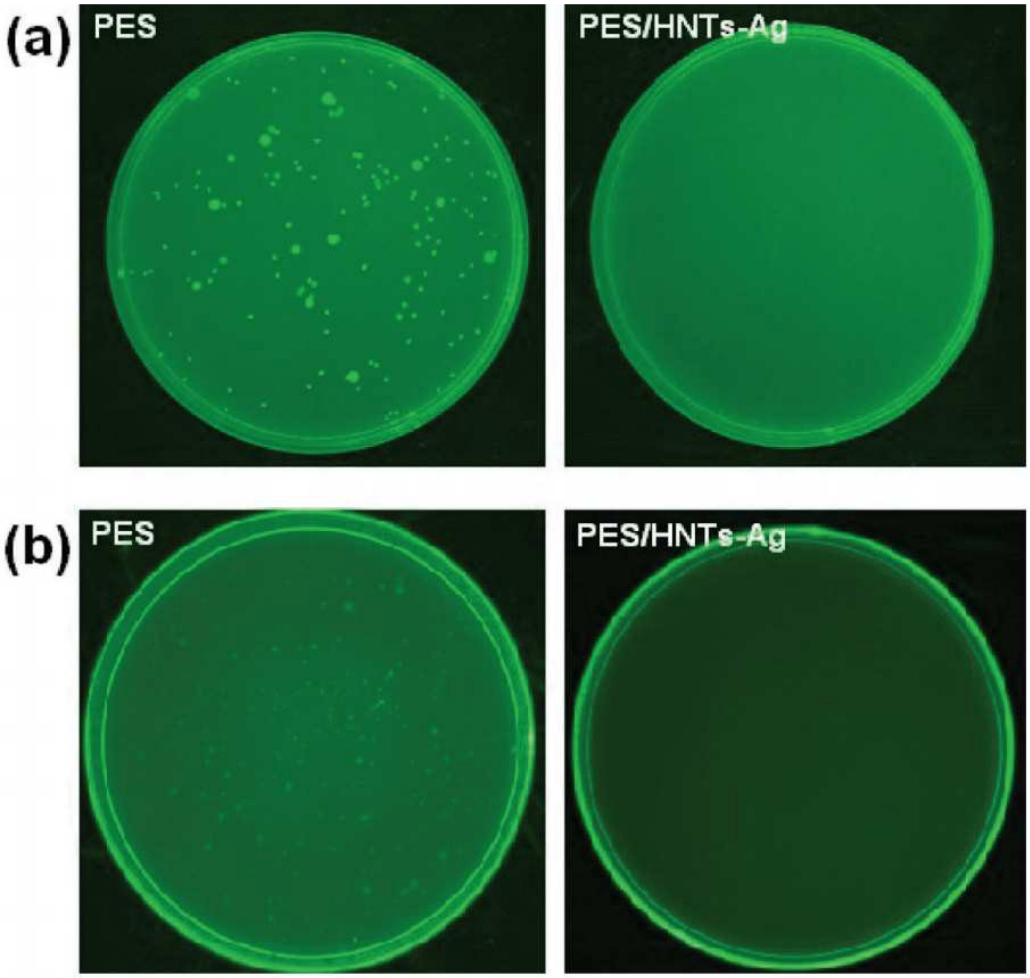

Fig. 17 Photographs showing the bacterial culture plates of (a) *E. coli* and (b) *S. aureus* to PES and PES/HNTs-AgNPs membranes [80]

Environmental Science: Nano Accepted Manuscript

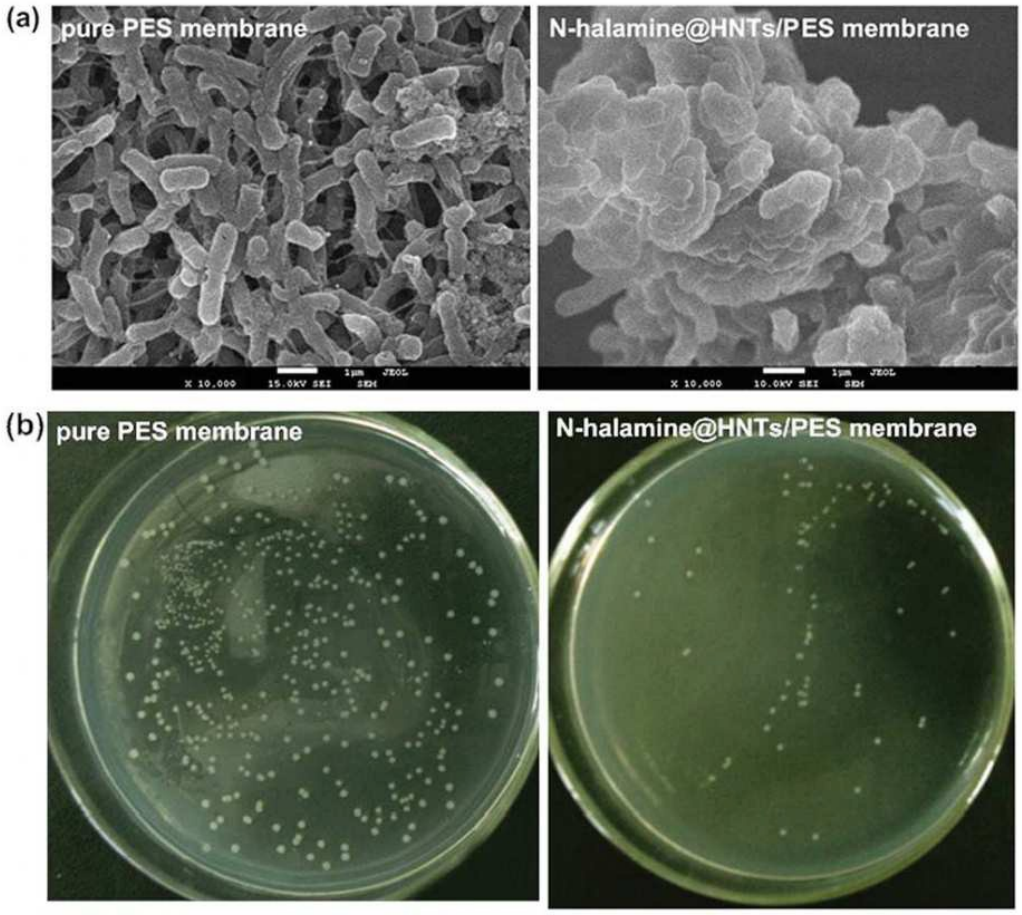

Fig. 18 (a) SEM images of E. coli attached to PES membrane and N-halamine@HNTs/PES membrane; (b) Bacteriostasis rate measurement of PES membrane and N-halamine@HNTs/PES membrane [87]

Environmental Science: Nano Accepted Manuscript

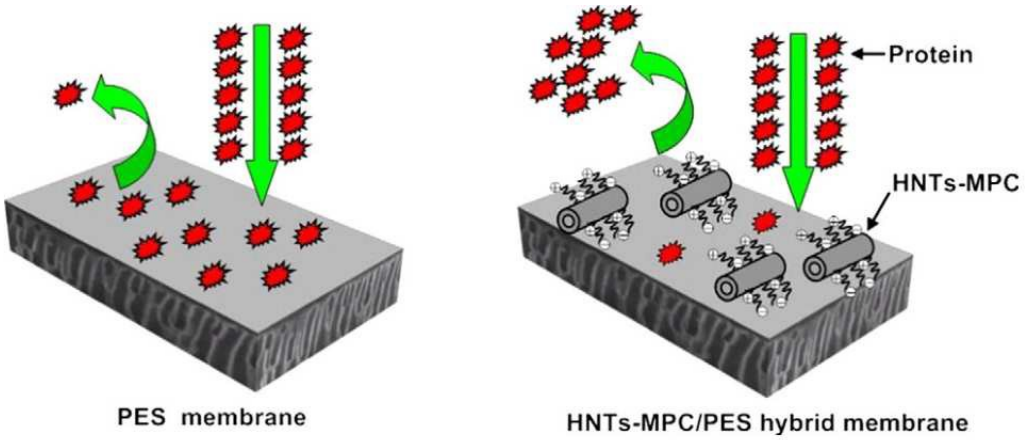

Fig. 19 Schematic diagram of HNTs-MPC/PES anti-protein-fouling ultrafiltration membrane [85]

Environmental Science: Nano Accepted Manuscript

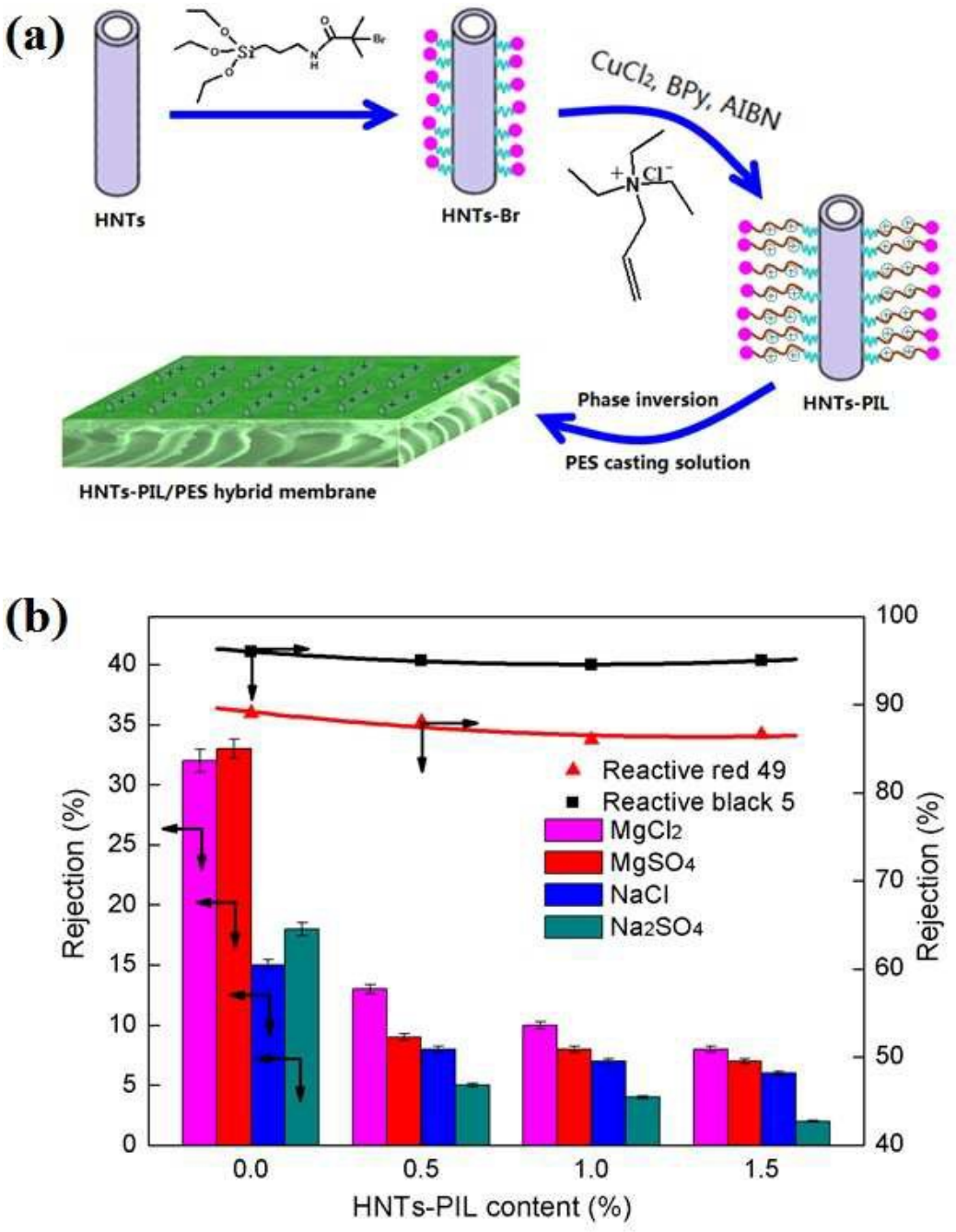

Fig.20 (a) Schematic showing fabrication process of HNTs-PIL/PES positively charged nanofiltration membrane and (b) rejections for dyes and salts of HNTs-PIL/PES membranes as a function of HNTs-PIL content [90]

Environmental Science: Nano Accepted Manuscript

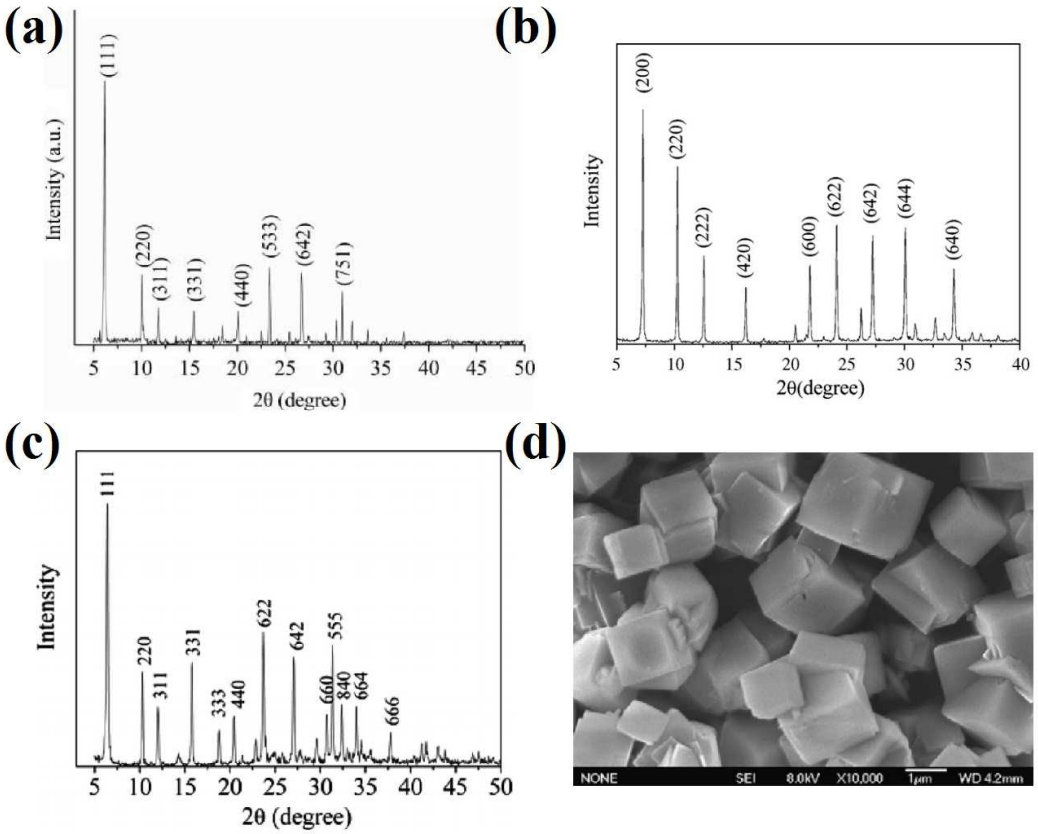

Fig. 21 XRD patterns of (a) zeolite X, (b) NaA zeolite, (c) zeolite Y and (d)SEM image of NaA zeolite synthesized from natural HNTs [101-104]

Environmental Science: Nano Accepted Manuscript

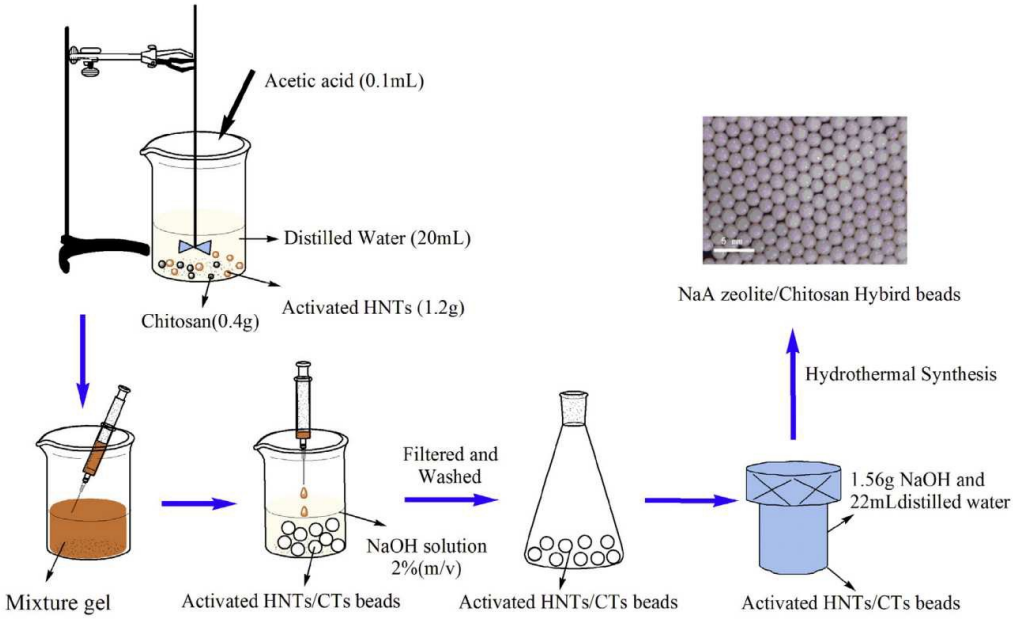

Fig. 22 Schematic showing the fabrication process of NaA zeolite/chitosan hybrid beads [103]

Environmental Science: Nano Accepted Manuscript

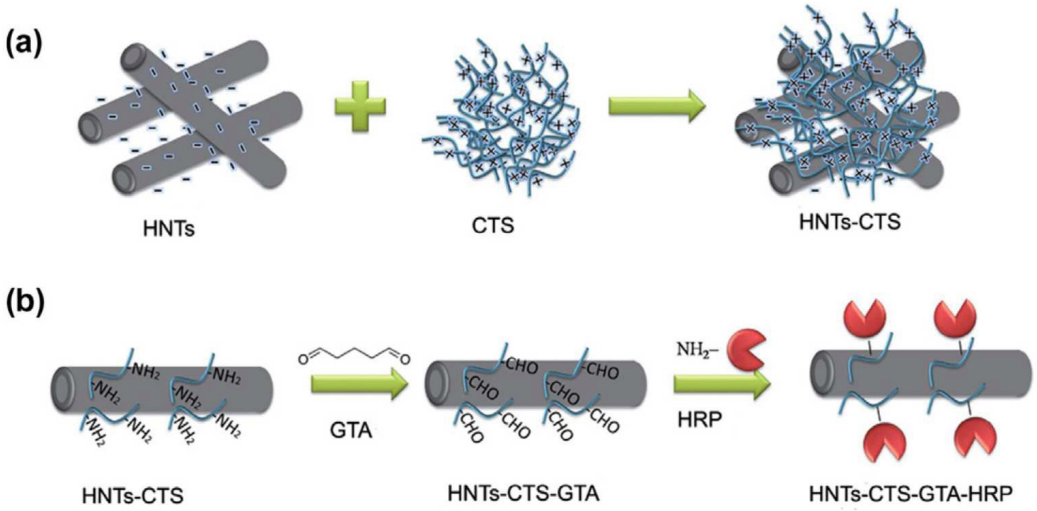

Fig. 23 Schematic illustration of (a) preparation of chitosan-halloysite hybrid nanotubes and (b) immobilization of horseradish peroxidase [107]

Environmental Science: Nano Accepted Manuscript